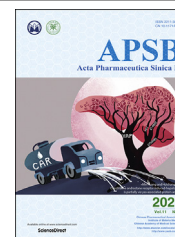




Chinese Pharmaceutical Association
Institute of Materia Medica, Chinese Academy of Medical Sciences

Acta Pharmaceutica Sinica B

www.elsevier.com/locate/apsb
www.sciencedirect.com



ORIGINAL ARTICLE

A novel SIRT6 activator ameliorates neuroinflammation and ischemic brain injury via EZH2/FOXC1 axis



Tailin He^{a,†}, Jialin Shang^{b,†}, Chenglong Gao^a, Xin Guan^a,
Yingyi Chen^b, Liwen Zhu^c, Luyong Zhang^a, Cunjin Zhang^{c,*},
Jian Zhang^{b,*}, Tao Pang^{a,*}

^aState Key Laboratory of Natural Medicines, Jiangsu Key Laboratory of Drug Screening, Jiangsu Key Laboratory of Drug Discovery for Metabolic Diseases, China Pharmaceutical University, Nanjing 210009, China

^bMedicinal Bioinformatics Center, Shanghai Jiao Tong University School of Medicine, Shanghai 200025, China

^cDepartment of Neurology of Drum Tower Hospital, Medical School and the State Key Laboratory of Pharmaceutical Biotechnology, Nanjing University, Nanjing 210008, China

Received 16 June 2020; received in revised form 26 August 2020; accepted 7 September 2020

KEYWORDS

SIRT6 activator;
Neuroinflammation;
Ischemic stroke;
Deacetylation;
Microglia;
Macrophage;
FOXC1;
EZH2

Abstract Ischemic stroke is the second leading cause of death worldwide with limited medications and neuroinflammation was recognized as a critical player in the progression of stroke, but how to control the overactive neuroinflammation is still a long-standing challenge. Here, we designed a novel SIRT6 activator MDL-811 which remarkably inhibited inflammatory response in lipopolysaccharide (LPS)-stimulated RAW264.7 macrophages and primary mouse microglia, which were abolished by silencing SIRT6. RNA-seq screening identified the forkhead box C1 (*Foxc1*) is a key gene evoked by MDL-811 stimulation and is required for the anti-inflammatory effects of MDL-811. We found MDL-811-activated SIRT6 directly interacted with enhancer of zeste homolog 2 (EZH2) and promoted deacetylation of EZH2 which could bind to the promoter of *Foxc1* and upregulate its expression to modulate inflammation. Moreover, our data demonstrated that MDL-811 not only ameliorated sickness behaviors in neuroinflammatory mice induced by LPS, but also markedly reduced the brain injury in ischemic stroke mice in addition to promoting long-term functional recovery. Importantly, MDL-811 also exhibited strong anti-inflammatory effects in human monocytes isolated from ischemic stroke patients, underlying an interesting translational perspective. Taken together, MDL-811 could be an alternative therapeutic candidate for ischemic stroke and other brain disorders associated with neuroinflammation.

*Corresponding authors. Tel./fax: +86 25 83271142 (Tao Pang), +86 21 64154900 (Jian Zhang), +86 25 83105921 (Cunjin Zhang).

E-mail addresses: tpang@cpu.edu.cn (Tao Pang), jian.zhang@sjtu.edu.cn (Jian Zhang), zhangcj@nju.edu.cn (Cunjin Zhang).

[†]These authors made equal contributions to this work.

Peer review under responsibility of Chinese Pharmaceutical Association and Institute of Materia Medica, Chinese Academy of Medical Sciences.

<https://doi.org/10.1016/j.apsb.2020.11.002>

2211-3835 © 2021 Chinese Pharmaceutical Association and Institute of Materia Medica, Chinese Academy of Medical Sciences. Production and hosting by Elsevier B.V. This is an open access article under the CC BY-NC-ND license (<http://creativecommons.org/licenses/by-nc-nd/4.0/>).

© 2021 Chinese Pharmaceutical Association and Institute of Materia Medica, Chinese Academy of Medical Sciences. Production and hosting by Elsevier B.V. This is an open access article under the CC BY-NC-ND license (<http://creativecommons.org/licenses/by-nc-nd/4.0/>).

1. Introduction

Stroke is an acute cerebrovascular disease caused by cerebral thrombosis or embolism¹, including hemorrhagic stroke and ischemic stroke, the latter accounting for 60%–80%. Ischemic stroke is one of the most serious diseases all over the world that seriously endangers human health and life safety. It has the characteristics of high morbidity, high disability, high recurrence rate and high mortality². The pathological process of ischemic brain injury is extremely rapid once it occurs. Currently, resolution of blood flow timely is the only therapeutic strategy and recombinant tissue plasminogen activator (r-tPA) is the only U.S. Food and Drug Administration (FDA)-licensed drug for the treatment of ischemic stroke³. However, ischemia/reperfusion (I/R) injury may aggravate the brain tissue damage and r-tPA has a number of limitations such as short time window and side effects. It is essential for us to get to know the pathophysiology and novel therapeutic targets of stroke in order to broaden our interventional options in this setting.

Several lines of evidence have suggested that microglia critically promote neuroinflammation after ischemia^{4–6}. Microglia are brain-resident macrophages which are originated from the embryonic yolk sac and then migrate to the central nervous system, becoming resident immune cells⁷. Under normal conditions, resting microglia are regulated by various signaling pathways and play an essential role in maintaining microenvironment homeostasis in brain. With the development of ischemic stroke, the homeostasis is broken, which causes continuous and excessive activation of microglia to release a large number of pro-inflammatory factors (tumor necrosis factor- α [TNF- α], interleukin [IL-1 β], inducible nitric oxide synthase [iNOS], etc.), nitric oxide and reactive oxygen species (ROS) within a few minutes after ischemia⁸, leading to destruction of the blood–brain barrier, brain edema and massive neuronal death⁹. On the other hand, activated microglia could also secrete anti-inflammatory mediators such as IL-10, arginase1 and TGF- β , growth and trophic factors such as insulin like growth factor 1 (IGF-1), nerve growth factor (NGF), and brain derived neurotrophic factor (BDNF), in addition to removing necrotic cells and phagocytose debris¹⁰. Compelling evidence has implicated regulation of microglial immune function, a vital contributor to the inflammation in the pathogenesis of ischemic stroke, is expected to further improve the prognosis of ischemic brain injury.

Chromatin regulation strongly impacts on modulation of inflammatory gene expression under various physio-pathological conditions. Sirtuins are a family of class III histone deacetylases (HDACs) and play an essential role in regulating the lifespan of mammals¹¹. N-terminal histone tails are susceptible to various reversible post-translational modifications, including acetylation, methylation, phosphorylation, ubiquitination and sumoylation¹². The 7 members of sirtuins (SIRT1–SIRT7) exhibit various nicotinamide adenosine dinucleotide (NAD⁺) dependent deacetylation activities by distinct substrates. Since

acetylation is one of the well-studied post-translational modifications of proteins, sirtuins play a determining role in many biological processes such as DNA repair, cell metabolism, and apoptosis^{13–15}. Among sirtuins, SIRT6 is tightly associated with chromatin and catalyzes the deacetylase of histone H3 lysine 9 (H3K9) and H3 lysine 56 (H3K56)¹⁶. Moreover, SIRT6 could also deacetylate forkhead box protein O1 (FOXO1)¹⁷, nuclear factor (erythroid-derived 2)-like 2 (NRF2)¹⁸, and other non-histone proteins. SIRT6 not only regulates mammals' aging but also participates in the inflammation^{19,20}, such as the secretion of TNF- α . SIRT6 is highly expressed in the brain and decreased SIRT6 expression was associated with enhanced production of inflammatory factors, such as high mobility group B1 (HMGB1) on ischemic stroke²¹. In addition, SIRT6 deficiency could also delay wound healing in mice by modulating inflammation and macrophage phenotypes²². Prognosis of ischemic brain injury alters gene expressions through neuroinflammation-induced chromatin changes²³. In particular, there is at best a limit understanding of SIRT6 in regulating neuroinflammation after ischemic stroke. Given that microglia and infiltrating macrophages are the main players in the neuroinflammation after ischemia and SIRT6 is highly expressed in both immune cells, we speculate that activating SIRT6 with our newly designed small-molecule activators might play an anti-neuroinflammatory role in ischemic stroke and produce beneficial outcomes after ischemic stroke.

Forkhead family is composed of a diverse group of transcription factors and has been increasingly regarded as a key participant in immune homeostasis²⁴. Among them, forkhead box C1 (FOXO1) has a transcriptional inhibitory domain which is closely related to various pathophysiological processes, such as oxidative stress²⁵, apoptosis²⁶ and inflammation²⁷. *Foxo1* gene is correlated to polycomb group proteins, especially enhancer of zeste homolog 2 (EZH2), whose acetylation results in target genes suppression²⁸. As one of the components of the polycomb repressor complex 2 (PRC2), it has been demonstrated that EZH2 is a critical epigenetic modifier that induces the trimethylation of H3K27 and is modulated by deacetylation of SIRT1²⁹. However, whether EZH2 could be deacetylated by SIRT6 to regulate FOXO1 to show an anti-inflammation role remains unknown and requires further investigations.

In the present study, we investigated, for the first time, whether our newly designed novel SIRT6 activators MDL-800 and MDL-811 have anti-neuroinflammatory function. Our results suggested that better than MDL-800, MDL-811 targeting SIRT6 remarkably ameliorated neuroinflammation and brain ischemic injury, and significantly promoted neurologic functional recovery by modulating microglia/macrophage activation. Furthermore, these beneficial effects were mediated by deacetylation of EZH2 and further activation of its target gene *Foxo1*. Importantly, SIRT6 activator MDL-811 suppressed inflammatory responses in human monocytes isolated from ischemic stroke patients, highlighting its potential translational value.

2. Materials and methods

2.1. Cell culture and drug treatment

RAW264.7 cells (American Type Culture Collection, ATCC, TIB-71), murine macrophage cells were cultured in DMEM (HyClone, Logan, UT, USA) containing 10% fetal bovine serum (Gibco, Carlsbad, CA, USA) at 37 °C in an atmosphere of 5% CO₂ and 95% air (Thermo Fisher Scientific, Waltham, MA, USA). The cells were seeded onto 96-well plates, 24-well plates, or 6-well plates after the density of cells reached 80% for further experiments.

Mouse primary cortical microglia were obtained from 24 to 48 hour-old C57BL/6 mice pups as we previously reported³⁰. Briefly, 24–28 hour-old mice pups' forebrains were dissected out on ice. After meninges and choroid plexus membranes were removed, forebrains were minced followed by digestion and cells were dissociated by various times of pipetting. Cells were seeded in 75 cm² flasks and were cultured in DMEM/F12 medium (HyClone) containing 10% fetal bovine serum at 37 °C in an atmosphere of 5% CO₂ and 95% air. Change culture medium on Days 3 and 6, and floating microglia can be collected from culture medium by shanking flasks on Day 9. Microglia were seeded onto 96-well plates or 24-well plates coated with poly-L-lysine (Sigma–Aldrich, Saint Louis, MO, USA) for further experiments.

Microglia or macrophages were incubated with various concentrations of MDL-800 or MDL-811 dissolved in DMSO (Sigma–Aldrich) for 2 h followed by treatment of 100 ng/mL of lipopolysaccharide (LPS, Sigma–Aldrich, dissolved in normal saline) for another 2 h, or followed by exposure to 3 h of the oxygen and glucose deprivation (OGD) to determine the gene and protein expressions of proinflammatory factors, or for another 12 h to determine the gene and protein expressions of anti-inflammatory factors.

2.2. Human samples collection

All the human subjects recruited to this study were approved by local ethics committee of the Affiliated Drum Tower Hospital of Nanjing University Medical School, Nanjing, China. Informed consent was obtained from all subjects. Blood was drawn at Day 6 after disease onset from 7 firstly diagnosed ischemic stroke patients without any immune interventions. Seven age- and gender-matched healthy subjects were recruited as controls. All the subjects neither received any immune-suppressive treatments in the recent one month, nor had any immunological or inflammatory disorders. Human peripheral blood monocytes were isolated by the adherence separation method. Peripheral blood mononuclear cells (PBMC) were isolated using a PBMC separation kit (Famacs, Nanjing, China) according to manufacturer's instructions. PBMCs were seeded onto 24-well plates and cultured in 1640 medium (HyClone) containing 10% fetal bovine serum at 37 °C in an atmosphere of 5% CO₂ and 95% air. Culture medium were replaced by fresh 1640 complete medium after 2 h to continue culturing adherent cells, most of which (>90%) were monocytes as detected by flow cytometry and subjected for further experiments. Monocytes were incubated with 1 μmol/L of MDL-811 dissolved in DMSO for 2 h followed by treatment of 50 ng/mL LPS (dissolved in normal saline) for another 2 h to determine the gene and protein expressions of inflammatory mediators.

2.3. SIRT6 protein purification and Fluor de Lys assay (FDL)

Wild-type SIRT6 protein was purified as previously described methods³¹. The full-length human SIRT6 was inserted into the pET28a-LIC vector, and the plasmids were transformed into *Escherichia coli* BL21 (DE3) cells. Protein was purified with a nickel column and gel filtration. Subsequently, the purified SIRT6 protein was dialyzed into the assay buffer (50 mmol/L Tris-HCl [pH 8.0], 137 mmol/L NaCl, 2.7 mmol/L KCl, and 1 mmol/L MgCl₂) and utilized in FDL assays. Wild-type SIRT6 protein (5 μmol/L) was incubated in a 50 μL of reaction mixture (DMSO/MDL-800/MDL-811, 2.5 mmol/L NAD⁺, 75 μmol/L RHKK-Ac-AMC, and assay buffer) at 37 °C for 2 h. Nicotinamide (40 mmol/L) was used as stop solution and the reaction system was continuously incubated with 6 mg/mL of trypsin at 25 °C for 30 min. Fluorescence intensity was assessed with a microplate reader (BD, Franklin Lakes, NJ, USA) at excitation and emission wavelengths of 360 and 460 nm respectively. EC₅₀ values were calculated by fitting the data points with the dose–response variable slope (four parameters) function in GraphPad Prism 5.

2.4. Molecular docking

Molecular docking calculations were performed using the crystal structure of SIRT6 (Protein Data Bank [PDB] code 5Y2F)³¹ in complex with MDL-811 and protein preparation was performed using the Protein Preparation Wizard in MAESTRO v11.2.013 (Schrödinger, Inc.). In addition, the compound was processed by the LigPrep module for 3D structure generation, protonation, and energy minimization. Subsequently, MDL-811 was docked into the allosteric site on SIRT6 to pick out the best binding mode defined by a 15 × 15 × 15 grid box implemented by GLIDE version 4.5.

2.5. Lipopolysaccharide (LPS)-induced inflammatory response model in RAW264.7 cells, primary mouse microglia and primary human monocytes

Cells were treated with MDL-811 dissolved in DMSO (Sigma–Aldrich) for 2 h followed by treatment with LPS (Sigma–Aldrich, 100 ng/mL) for another 2 or 12 h. The cell culture media were collected after centrifugation and total proteins and RNA were isolated as we reported previously³² for further experiments.

2.6. Oxygen-glucose deprivation

Primary mouse microglia were seeded onto 24-well plates pre-coated with poly-L-lysine at the density of 5 × 10⁴/well. After 24 h fusion, cells were treated with MDL-811 dissolved in DMSO (Sigma–Aldrich) for 2 h and then culture media were replaced into glucose-free DMEM (HyClone), and the plates were placed into a tri-gas incubator with 94% N₂, 5% CO₂ and 1% O₂ mixture to expel oxygen for 3 h. Cells treated with glucose-free DMEM plus D-glucose (3151 mg/L) and incubated in the normal condition were used as control. The cell culture media were collected after centrifugation and total proteins and RNA were isolated as we reported previously³² for further experiments.

2.7. Enzyme-linked immunosorbent assay (ELISA)

Mouse TNF- α ELISA kit (EK0527, BOSTER Biological Technology, Pleasanton, CA, USA) was used to detect the concentration of TNF- α in the cell culture media or mice according to the manufacturer's instructions.

2.8. Western blot analysis

Protein isolation from whole cerebral cortex or cells was performed as described previously³³. The concentration of protein was assessed by BCA assay kit (Thermo Fisher). Western blots were performed using the standard SDS-polyacrylamide gel electrophoresis method and electrotransferred onto PVDF membranes (Millipore, Billerica, MA, USA). After blocking with 3% (*w/v*) BSA (SunShine, Nanjing, China) in PBS for 2 h, the membranes were incubated with primary antibodies at 4 °C overnight, and then incubated with the corresponding secondary antibodies (CST, Boston, MA, USA; 1:10,000) for 1 h at room temperature. At last, the immunoblot was visualized and quantified by a gel densitometric scanning and analysis system (Bio-Rad, Berkeley, CA, USA).

Primary antibodies were used as follows: anti-SIRT6 (#12486; CST; 1:1000), anti-H3K9Ac (#9469; CST; 1:1000), anti-H3K56Ac (#4232; CST; 1:1000), anti-EZH2 (#5246; CST; 1:1000), anti-FOXC1 (ab227977; abcam, Cambridge, UK; 1:1000), anti-Pan Ac-K (A2391; abclonal, Wuhan, Hubei, China; 1:1000), anti-H3K14Ac (A7254; abclonal; 1:1000), anti-H3K27me3 (A2363; abclonal; 1:1000), anti-Histone H3 (BS90642; Bioworld Technology, Louis Park, MN, USA; 1:1000), anti- β -Actin (23660-1-AP; Proteintech, Wuhan, Hubei, China; 1:10,000).

2.9. Real-time quantitative polymerase chain reaction

One microgram of RNA was reverse transcribed with the HiScript Q RT SuperMix for qPCR (Vazyme, Nanjing, Jiangsu, China). cDNA was analyzed by qPCR using the SYBR qPCR Master Mix (High ROX Premixed, Vazyme), a CFX384 real-time System C1000 Thermal Cycler (Bio-Rad) and the Bio-Rad CFX Manager 3.1 software. The reaction conditions were as follows: 95 °C for 10 min followed by 40 cycles of 95 °C for 10 s and 60 °C for 1 min. The relative amount of the different mRNAs was quantified with the $\Delta\Delta$ Ct method with 18S rRNA as normalization. The information of the primers is described in Supporting Information Table S1.

2.10. Cell transfection

To facilitate the knockdown of SIRT6 or FOXC1 expression, we transfected a *Sirt6* or *Foxc1* gene siRNA (20 nmol/L) as well as the corresponding negative controls into RAW264.7 cells or mouse primary cortical microglia for 36 h using Lipofectamine 3000 (Invitrogen, Carlsbad, CA, USA) according to the manufacturer's instructions. The information of the sequences of *Sirt6* and *Foxc1* gene siRNAs is described in Supporting Information Table S2.

2.11. mRNA sequencing

RAW264.7 cells were treated with MDL-811 (5 μ mol/L) or DMSO for 3 h, then the cells were treated with LPS (100 ng/mL)

for another 2 h. After the treatment, all the samples were sequenced by the Solexa high-throughput sequencing service (Obiotech, Shanghai, China). Total RNAs were obtained using an RNeasy Mini kit (Qiagen, Valencia, CA, USA) and the concentration and quality were detected with Nanodrop 2000 (Thermo Fisher Scientific) and Agilent 2100 Bioanalyzer (Agilent, Santa Clara, CA, USA). A total of 50 ng RNA was sequenced by HiSeqTM 2500 (Illumina, San Diego, CA, USA). $P < 0.05$ and fold change >2 or <0.5 was considered as significant difference. All differentially expressed gene lists ($P < 0.05$) generated by DESeq56 were subsequently analyzed for enrichment of biological terms with the Database for Annotation, Visualization and Integrated Discovery (DAVID) bioinformatics platform. Gene expression patterns were analyzed by hierarchical cluster analysis and volcano plots. KEGG pathway enrichment analysis of differentially expressed transcripts was performed using R based on the hypergeometric distribution. RNA sequencing raw data has been uploaded to SRA database whose accession numbers are as follows: Sample_CN_1 SRR11069607, Sample_CN_2 SRR11069606, Sample_CN_3 SRR11069605, Sample_ZJ_011_1 SRR11069604, Sample_ZJ_011_2 SRR11069603, Sample_ZJ_011_3 SRR11069602.

2.12. Immunoprecipitation and immunoblotting

RAW264.7 cells were lysed using IP Lysis Buffer (Solarbio, Beijing, China) containing protease inhibitor cocktail (Selleckchem, Houston, TX, USA). Lysates were precleared using protein A+G agarose (Beyotime, Shanghai, China). Samples were immunoprecipitated using anti-EZH2 antibody (CST; 1:100) overnight at 4 °C, and immunoprecipitates were collected on beads for 4 h. Beads were washed in IP lysis buffer containing protease inhibitor cocktail for 3 times. 4 \times Laemmli sample buffer (Bio-Rad) was then added to the beads, and samples were boiled, separated by SDS-PAGE, and immunoblotted as described previously³⁴.

2.13. Chromatin immunoprecipitation (ChIP) assay

RAW264.7 cells were crosslinked with 1% (*v/v*) formaldehyde and were subjected to ChIP assays using Chromatin IP Assay Kit (Millipore). Briefly, cells were lysed and then sonicated to obtain DNA fragments (200–1000 bp in size) using an ultrasonic cell disruptor (Branson, Danbury, CT, USA). The soluble chromatin was then immunoprecipitated with anti-FOXC1 antibody (ab5079; Abcam; 1:50) overnight at 4 °C with rotation and then supplemented with protein A agarose/salmon sperm DNA for 1 h at 4 °C. Reversing the cross-links was carried out for 4 h at 65 °C. DNA was purified with a DNA extraction kit (Qiagen). Finally, the purified DNA was analyzed by qPCR. Primers for qPCR are listed in Table S1. P1–P3 denote the three promoter regions of *Foxc1* gene analyzed in ChIP assays, and P4 is at the distal region²⁸.

2.14. Animals

Male ICR mice aged 8–10 weeks, weighing 22–26 g, were purchased from Zhejiang Laboratory Animals Center (Hangzhou, Zhejiang, China) and kept under standard housing conditions at a temperature between 24 and 26 °C, with a 12 h light–dark cycle and a relative humidity between 40% and 60%. All procedures were performed following institutional approval in accordance with the NIH Guide for the Care and Use of Laboratory Animals published by the US National Academy of Sciences (<http://oacu>).

od.nih.gov/regis/index.htm). All animal tests and experimental procedures were approved by the Administration Committee of Experimental Animals in Jiangsu Province and the Ethics Committee of China Pharmaceutical University, Nanjing, China.

2.15. Lipopolysaccharide (LPS)-induced neuroinflammation model in mice

A diagram of the experimental design is shown in the Supporting Information Fig. S1A. Twenty four mice were randomly assigned to experimental groups (Control, LPS+vehicle, LPS+MDL-811 [1 mg/kg], LPS+MDL-811 [10 mg/kg], 6 mice in each group) and were intravenously administered with MDL-811 (1 or 10 mg/kg) or the vehicle (1% DMSO in normal saline) for 3 consecutive days daily. The dosage of MDL-811 was 1 or 10 mg/kg and the injection volume was 4 mL/kg. In the vehicle control group, an equal volume of the vehicle was administered by the same regimen. On the Day 4, mice were intraperitoneally administered with LPS (Sigma–Aldrich, 0.33 mg/kg) or the vehicle (normal saline) for 3 h. Total proteins and RNA isolation from whole cerebral cortex and serum of mice were collected after the mice were sacrificed under deep anesthesia for further experiments.

2.16. Locomotor activity determination

Open field test was utilized to determine locomotor activity after mice were subjected to LPS for 3 h. Mice were gently placed into the center of the open field box (ZS Dichuang, Beijing, China) and the total distance travelled and time spent in the inner and outer zones were measured for 5 min. These were recorded by an overhead camera and analyzed with TopScan software (Any-maze™, Stoelting Co.). Total distance, line crossings, time/distance in the central zone were recorded and analyzed.

2.17. Focal cerebral ischemia/reperfusion and drug treatment

A diagram of the experimental design is shown in Fig. S1B and S1C. Transient middle cerebral artery occlusion (tMCAO) was performed to get a focal cerebral ischemia/reperfusion model in mice. Seventy-three mice were randomly assigned into experimental groups (acute tMCAO experiment: 8 in sham group, 12 in tMCAO+vehicle group, 10 in tMCAO+MDL-811 [1 mg/kg] group, and 10 in tMCAO+MDL-811 [10 mg/kg] group; chronic tMCAO experiment: 8 in sham group, 14 in tMCAO+vehicle group, 13 in tMCAO+MDL-811 group). Mice were anesthetized with 3% isoflurane and maintained at 1%–2% isoflurane during the surgery. Body temperature was maintained at 37 ± 0.5 °C with a surface heating pad during the surgery. Focal cerebral ischemia/reperfusion was induced by transient middle cerebral artery (MCA) occlusion for 45 min by inserting a silicone-coated nylon suture (Jialing Biotechnology, Guangzhou, China) into the right MCA *via* right external carotid artery (ECA) and internal carotid artery (ICA). The Laser Speckle Imaging (Gene & I, Beijing, China) was used to monitor the blood flow and when it decreased to more than 70% of the base line immediately, it was considered as a successful model (Supporting Information Fig. S6A). For the sham group, surgeries were conducted without nylon suture insertion into the right external carotid artery. During the acute tMCAO experiment (Fig. 6), a total of 40 mice were used and 8 mice were excluded because of unsuccessful model ($n = 2$) or sacrifice ($n = 6$). During the chronic tMCAO experiment (Fig. 7),

a total of 33 mice were used and 5 mice were excluded because of unsuccessful model ($n = 2$) or sacrifice in the operation ($n = 3$). Survival rate and survival time during the experiment were recorded and analyzed (Fig. S6D).

MDL-811 (dissolved in 1% of DMSO in normal saline) was administered intravenously to mice 1, 24 and 48 h after the surgery respectively. The dosage of MDL-811 was 1 or 10 mg/kg and the injection volume was 4 mL/kg. In the vehicle control group, an equal volume of the vehicle was administered by the same regimen. Total proteins and RNA isolation from peri-infarct cerebral cortex of mice were collected after the mice were sacrificed under deep anesthesia for further experiments.

2.18. Measurement of infarction size and neurological performance

Infarction size was detected by 2,3,5-triphenyltetrazolium chloride (TTC) staining. At 72 h after ischemia, the mice were deeply anesthetized with isoflurane and euthanized. The brains were coronally sectioned into 5 slices with 2 mm thickness, and then placed into 2% (*w/v*) TTC (Sigma–Aldrich) solution at 37 °C for 10 min. The infarction size of the slices was measured by NIH Image J software. To avoid the influence of cerebral edema, the infarction in each section was normalized to the non-ischemic contralateral side and expressed as a percentage of the contralateral hemisphere with Eq. (1):

$$\text{Infarct size (\%)} = (\text{Contralateral area} - \text{Ipsilateral non-infarct area}) / \text{Contralateral area} \times 100 \quad (1)$$

Modified Longa's method³⁵, modified neurological severity scores (mNSS) method³⁶ and corner test¹⁰ were used to evaluate the neurological performance as we have reported previously. The mice's neurological performance scores and the times of turning to right were recorded.

2.19. In vivo brain magnetic resonance imaging (MRI) scanning

In vivo brain MRI was performed using a 7.0 tesla small animal magnetic resonance scanner (PharmaScan 7T, Bruker, Carlsruhe, Germany). On the Day 14 after tMCAO, the infarct volume was calculated by T2-weighted images using a 2D fast-spin echo sequence (2500/33 ms of repetition time/echo time, 1 average). Mice were anesthetized with 3% isoflurane in an anesthesia induction box. After righting reflex was disappeared, mice were transferred onto the detector with 1.5% isoflurane delivered through a nose cone. Sixteen 1-mm-thick coronal slices, each with a 256×256 matrix and a 20×20 mm FOV, were positioned over the brain, excluding the olfactory bulb. To avoid the influence of cerebral edema, the infarction in each slice was normalized to the non-ischemic contralateral side and expressed as a percentage of the contralateral hemisphere with Eq. (1).

2.20. Immunofluorescence staining

At the end of the LPS-induced neuroinflammation study or 72 h after tMCAO, mice were euthanized with deep anesthesia (5% isoflurane) and then intracardially perfused with normal saline, followed by buffered paraformaldehyde (4%). The brains were collected and post-fixed in 4% paraformaldehyde for 24 h. Then the brains were transferred into 15% sucrose for 24 h and 30%

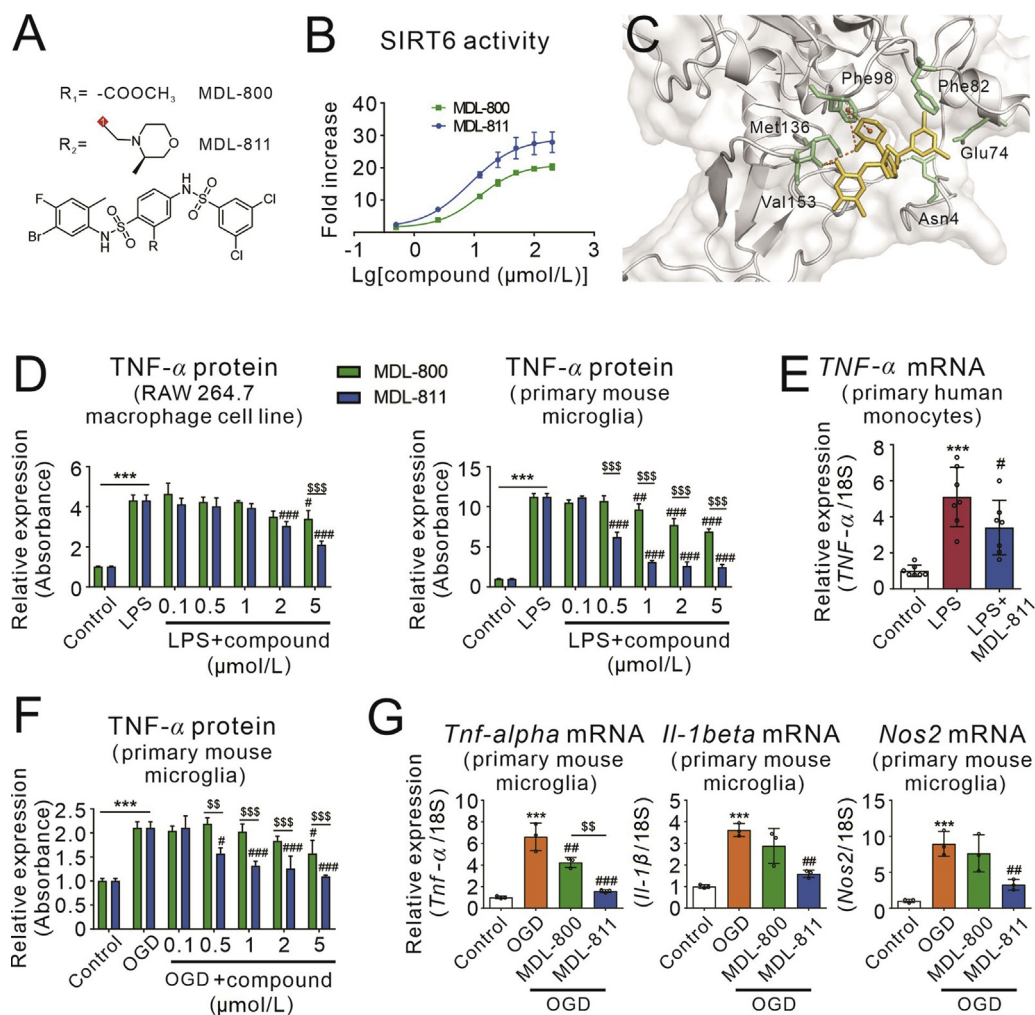


Figure 1 Discovery of MDL-811 as a superior SIRT6 activator with strong anti-inflammatory action. (A) Chemical structures of MDL-800 and MDL-811. (B) Dose–response of MDL-800 and MDL-811 on SIRT6 activation at the molecular level determined using FDL assays ($n = 3$) and MDL-811 shows more potent activity. Data are presented as means \pm SEM, representing three independent experiments. (C) View of the allosteric pocket of SIRT6 occupied by MDL-811. SIRT6 is displayed as a grey cartoon, and MDL-811 is displayed as yellow sticks. The residues within the binding site of MDL-811 are shown in the green sticks. Hydrogen bonds are indicated by dotted lines. (D) Dose-dependent manners of MDL-800 and MDL-811 in inhibiting LPS-induced TNF- α release in RAW264.7 cells and primary mouse microglia. Cells were incubated with various concentrations of MDL-800 or MDL-811 for 2 h followed by treatment of 100 ng/mL LPS for another 2 h, and TNF- α in the culture medium was detected using ELISA ($n = 3$). The experiments were repeated three times on different days. Results are expressed as means \pm SEM; *** $P < 0.001$ versus control group; # $P < 0.05$, ## $P < 0.01$, ### $P < 0.001$ versus LPS group; \$\$\$ $P < 0.001$, MDL-811 group versus MDL-800 group. (E) MDL-811 significantly reduced the TNF- α mRNA expression in LPS-stimulated primary normal human monocytes. Cells were incubated with 1 $\mu\text{mol/L}$ of MDL-811 for 2 h followed by stimulation with 50 ng/mL LPS for another 2 h ($n = 3$). The experiments were repeated three times on different days. Results are expressed as means \pm SEM; *** $P < 0.001$ versus control group; # $P < 0.05$ versus LPS group. (F) Dose-dependent manners of MDL-800 and MDL-811 in inhibiting the oxygen and glucose deprivation (OGD)-induced TNF- α release in primary mouse microglia. Cells were incubated with various concentrations of MDL-800 or MDL-811 for 2 h followed by exposure to 3 h of OGD, and TNF- α in the culture medium was detected using ELISA ($n = 3$). The experiments were repeated three times on different days. Results are expressed as means \pm SEM; *** $P < 0.001$ versus control group; # $P < 0.05$, ### $P < 0.001$ versus the OGD group; \$\$\$ $P < 0.01$, \$\$\$ $P < 0.001$, MDL-811 group versus the MDL-800 group. (G) MDL-811 significantly reduced the mRNA expression of proinflammatory genes (*Tnf- α* , *Il-1 β* , and *Nos2*) in primary mouse microglia under OGD condition. Cells were incubated with 1 $\mu\text{mol/L}$ of MDL-800 or MDL-811 for 2 h followed by exposure to 3 h of OGD to test the mRNA expression level of proinflammatory factors ($n = 3$). The experiments were repeated three times on different days. Results are expressed as means \pm SEM; *** $P < 0.001$ versus control group; ## $P < 0.01$, ### $P < 0.001$ versus OGD group; \$\$\$ $P < 0.01$, MDL-811 group versus MDL-800 group.

sucrose for another 24 h. The brain blocks (+1.18 to -0.10 mm from bregma) were sliced into 16 μm -thick coronal sections with a microtome (CM3050S, Leica, Wetzlar, Germany). The sections were washed with 0.3% TritonX-100 in PBS and blocked with 1%

BSA in 0.3% TritonX-100/PBS for 2 h at room temperature. Next, the sections were incubated with rabbit anti-IBA1 antibody (019-19741; Wako, Osaka, Japan; 1:500) and rat anti-CD16 antibody (553142; BD biosciences; 1:100) in 1% BSA in 0.3% TritonX-

100/PBS at 4 °C overnight. Sections were then incubated with fluorescent conjugated secondary antibodies. Images were captured using a fluorescence microscope (FV3000, Olympus, Tokyo, Japan). The numbers of stained target cells were quantified using Image J software. Three random microscopic fields on the cortex of each section were analyzed. Immunostaining target cell counts were expressed as the average numbers of cells per square millimeter.

2.21. Statistical analysis

The data in this study are represented as mean \pm standard error of mean (SEM) and calculated using GraphPad Prism 5. Statistical analysis among the frequencies (modified Longa test, mNSS test and corner test) were carried out using non-parametric Mann–Whitney test, and two groups comparisons were carried out using the unpaired 2-tailed Student's *t* test and multiple groups comparisons were carried out using the One-way ANOVA followed by Bonferroni's test or using the Two-way ANOVA followed by Bonferroni's test. $P < 0.05$ was considered statistically significant.

3. Results

3.1. Discovery of MDL-811 as a superior SIRT6 activator with strong anti-inflammation in microglia/macrophages

SIRT6 plays an essential role in the pathogenesis of systemic inflammation²² but whether SIRT6 regulates neuroinflammation remains unknown. SIRT6 activator could be used as a pharmacological tool to investigate its role in neuroinflammation. We discovered MDL-800 compound as a first-in-class small-molecule SIRT6 activator and MDL-811 is an improved SIRT6 activator with a half-maximal effective concentration (EC₅₀) value of 7.09 ± 0.88 $\mu\text{mol/L}$ (Fig. 1A and B). According to our docking model, MDL-811 could form a hydrogen bond with Phe86 and take part in hydrophobic interactions with Phe86 and Val153, turning into binding sites of SIRT6 (Fig. 1C).

LPS is a well-documented bacterial endotoxin that releases pro-inflammatory cytokines such as TNF- α , IL-1 β and nitric oxide to induce inflammation in macrophages and microglia^{37,38}. In order to evaluate and compare the anti-inflammatory effects of both SIRT6 activators, various concentrations of MDL-800 or MDL-811 were used in LPS-stimulated RAW264.7 macrophage cell line and primary mouse microglia cells. MDL-800 and MDL-811 dose-dependently reduced release of TNF- α , an inflammatory cytokine in LPS-treated RAW264.7 cells and primary mouse microglia, while MDL-811 has a more potent anti-inflammation than MDL-800 (Fig. 1D). We further validated MDL-811 anti-inflammation effect in primary human monocytes. MDL-811 at 1 $\mu\text{mol/L}$ significantly reduced LPS-induced TNF- α mRNA expression in cultured normal human monocytes (Fig. 1E).

Microglia-mediated neuroinflammation aggravates brain ischemic injury. We then examined the role of MDL-800 and MDL-811 in oxygen-glucose deprivation (OGD)-induced microglia activation in primary mouse microglia to mimic neuroinflammation during the ischemic stroke *in vitro*. The results indicated that MDL-811 was dose-dependently decreased the release of TNF- α induced by OGD and it exhibited the optimum effect at the concentration of 1 $\mu\text{mol/L}$. On the contrary, MDL-800 did not show a favorable anti-inflammatory effect compared with

MDL-811 (Fig. 1F). We also evaluated the gene expression of various proinflammatory factors (Fig. 1G). MDL-811 (1 $\mu\text{mol/L}$) significantly reduced the gene expression of OGD-induced pro-inflammatory factors, including *Tnf- α* , *Il-1 β* and *Nos2*. However, MDL-800 did not show a favorable anti-inflammatory effect compared with MDL-811. Thus, we used 5 $\mu\text{mol/L}$ of MDL-811 in RAW264.7 cells and 1 $\mu\text{mol/L}$ of it in primary mouse microglia in the following experiments.

3.2. MDL-811 targeting SIRT6 modulates inflammatory response in LPS-stimulated primary mouse microglia and RAW264.7 macrophage cells

Since compound MDL-811 has a potent anti-inflammatory effect, we continued to explore whether it is related to SIRT6 activation. SIRT6 could catalyze the deacetylation of its substrate histone H3 lysine 9 (H3K9) and H3 lysine 56 (H3K56). To evaluate the SIRT6 activation by MDL-811, we monitored acetylated H3K9 (H3K9Ac) and acetylated H3K56 (H3K56Ac) protein levels in RAW264.7 macrophage cell line and primary mouse microglia after treated with MDL-811. As shown in Fig. 2A and E, Supporting Information Fig. S2A and S2C, it was observed that H3K9Ac and H3K56Ac were both decreased time-dependently in both cells after treated with MDL-811. However, SIRT6 was not markedly changed, suggesting that MDL-811 could promote SIRT6 activity by deacetylating H3K9 and H3K56. Remarkably, MDL-811 did not affect the SIRT1 substrate H3K14Ac protein levels, indicating that MDL-811 specifically activates SIRT6 in both cells.

Meanwhile, we investigated whether SIRT6 silencing would influence the anti-inflammatory effects of MDL-811 in both cells. In RAW264.7 macrophage cells and primary mouse microglia, MDL-811 markedly reduced the LPS-induced TNF- α release (Fig. 2C and G) and the pro-inflammatory genes expressions, including *Tnf- α* , *Il-1 β* , and *Nos2* (Fig. 2C and G, Fig. S2B and S2D) and significantly increased the anti-inflammatory genes expressions, including *arginase1*, *CD206* and *Il-10* (Fig. 2D and H, Fig. S2B and S2D). However, these anti-inflammatory effects were attenuated by SIRT6 silencing (Fig. 2B and F) with *Sirt6* siRNA (Fig. 2 and Fig. S2), suggesting that MDL-811 anti-inflammatory effects were mediated through SIRT6.

3.3. FOXC1 is involved in the anti-inflammation of MDL-811

To further clarify the potential mechanism of anti-inflammation effects of MDL-811, we analyzed the transcriptomes of MDL-811-treated/untreated RAW264.7 cells followed by LPS stimulation using RNA-seq. Hierarchical cluster analysis and the volcano diagram showed that out of more than 20,000 genes evaluated, a total of 72 and 269 genes were upregulated or downregulated, respectively (Fig. 3A and B). Subsequently, we conducted GO enrichment analysis and KEGG enrichment analysis. Interestingly, many of distinguishable gene patterns were correlated to inflammation. From the top 30 GO terms (Supporting Information Fig. S3A) and top 20 KEGG enrichment (Fig. 3C) screened out and KEGG pathway classification (Fig. S3B), we noticed that differential genes were strongly correlated to immune response and inflammatory response, many of which are a part of inflammatory pathways, such as TNF, JAK-STAT, NF- κ B, and MAPK. So we screened and validated the results by qPCR according to the data above in RAW264.7 cells. We found 8 genes were upregulated and 5 genes were downregulated by MDL-811 in RAW264.7 cells incubated

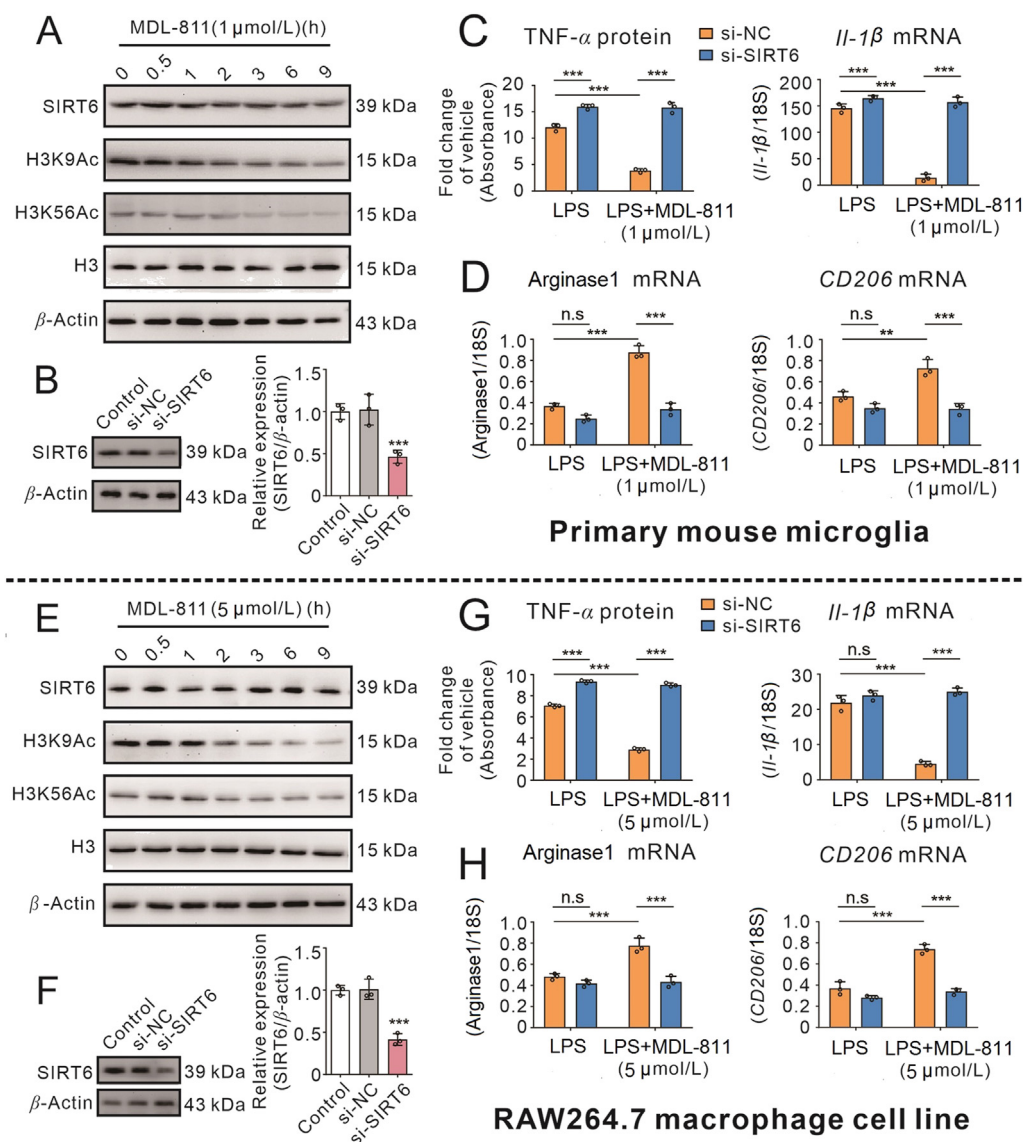


Figure 2 MDL-811 reduces inflammatory responses in both macrophages and microglia through SIRT6 activation. (A) and (E) Western blot analysis on expression of SIRT6, H3K9Ac, and H3K56Ac in primary mouse microglia or RAW264.7 cells incubated with MDL-811 for different time. H3 is the internal control and β -actin is the loading control. Data are representative of three independent experiments. (B) and (F) The expression of SIRT6 protein in primary mouse microglia or RAW264.7 cells transfected with 20 nmol/L *Sirt6* gene siRNA for 48 h ($n = 3$). Data are representative of three independent experiments. $***P < 0.001$ versus normal control siRNA (si-NC) group. (C) and (G) MDL-811 inhibited pro-inflammatory factors protein (TNF- α) or mRNA (*Il-1 β*) expression in LPS (100 ng/mL)-stimulated microglia or RAW264.7 cells, which were abolished by SIRT6 knockdown ($n = 3$). The q-PCR results were normalized to 18S rRNA. Results are expressed as means \pm SEM. Data are representative of three independent experiments; $***P < 0.001$. (D) and (H) MDL-811 promoted anti-inflammatory factors (arginase1, *CD206*) mRNA expressions in LPS-incubated microglia or RAW264.7 cells, which were abolished by SIRT6 knockdown ($n = 3$). The q-PCR results were normalized to 18S rRNA. Results are expressed as mean \pm SEM. Data are representative of three independent experiments; n.s.: not significant, $**P < 0.01$, $***P < 0.001$.

with LPS (Fig. S3C). However, MDL-811 alone treatment remarkably enhanced *Foxc1* gene expression in RAW264.7 cells (Fig. S3D). Furthermore, MDL-811 dose-dependently and time-dependently increased the gene expression of *Foxc1* in RAW264.7 and primary mouse microglia cells (Fig. 3D and G, Fig. S3E and G). Moreover, we investigated whether FOXC1 contributes to the anti-inflammatory effects of MDL-811 by *Foxc1* gene silencing. FOXC1 knockdown significantly reversed the MDL-811 inhibition of LPS-induced TNF- α release (Fig. 3E and H) and the gene expression of pro-inflammatory factors including *Tnf- α* , *Il-1 β* , and *Nos2* (Fig. 3F and Fig. S3F), and significantly

attenuated the gene expression of anti-inflammatory factors, including *CD206* (Fig. 3I and Fig. S3H) in RAW264.7 macrophage cells and primary mouse microglia cells.

3.4. SIRT6-mediated EZH2 deacetylation is involved in MDL-811 anti-inflammation

SIRT6 is a kind of deacetylase that regulates the transcription of its target genes by interacting with various transcription factors³⁹. Accumulating studies found that the acetylation of EZH2 enhances its capacity in regulating FOXC1^{28,40}. To determine

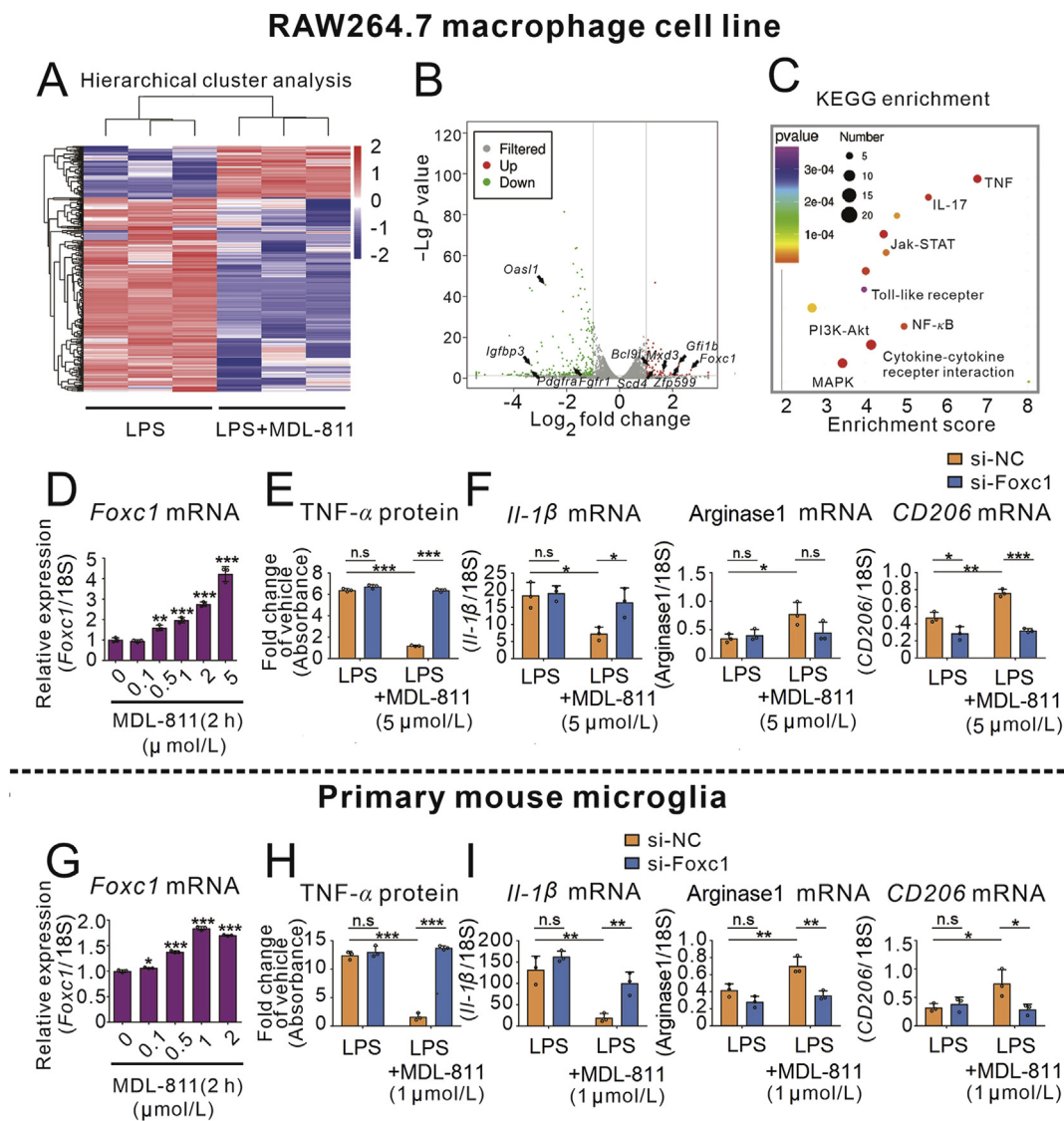


Figure 3 Transcriptomics reveals *Foxc1* gene involved in the MDL-811 anti-inflammation. (A) RNA sequencing cluster analysis chart. RAW264.7 cells were incubated with 5 $\mu\text{mol/L}$ of MDL-811 or DMSO followed with LPS (100 ng/mL) stimulation ($n = 3$). Pink indicates that genes were upregulated ($P < 0.05$ and fold change > 2), and blue indicates that genes were downregulated ($P < 0.05$ and fold change < 0.5) after the treatment of MDL-811. (B) The distribution of differentially expressed genes was displayed in the volcano diagram. The vertical grey lines represent fold change = 2 or 0.5, and the horizontal grey line represents $P = 0.05$. The red points display upregulated genes and the green points display downregulated genes after the treatment of MDL-811 ($n = 3$). (C) KEGG signaling pathways that were significantly changed after the treatment of MDL-811 ($P < 0.05$ and fold change > 2 or < 0.5). Different colors of bubbles represent the P value and the different sizes of bubbles represent the number of genes in the signaling pathway. (D) and (G) q-PCR analysis on *Foxc1* mRNA in RAW264.7 cells or primary mouse microglia incubated with various concentrations of MDL-811 for 2 h ($n = 3$). Results were normalized to 18S rRNA. Data are representative of three independent experiments. Results are expressed as mean \pm SEM; * $P < 0.05$, ** $P < 0.01$, *** $P < 0.001$. (E) and (H) FOXC1 knockdown reversed the MDL-811-mediated inhibition of *TNF- α* release in LPS-incubated RAW264.7 cells or primary mouse microglia ($n = 3$). Results are expressed as mean \pm SEM. Data are representative of three independent experiments; n.s.: not significant, *** $P < 0.001$. (F) and (I) FOXC1 knockdown reversed the MDL-811-mediated inhibition of pro-inflammatory factor *Il-1 β* mRNA expression and promotion of anti-inflammatory mediators (arginase1 and *CD206*) mRNA expressions in RAW264.7 cells or primary mouse microglia ($n = 3$). Results are expressed as mean \pm SEM. Results were normalized to 18S rRNA. Data are representative of three independent experiments; n.s.: not significant, * $P < 0.05$, ** $P < 0.01$, *** $P < 0.001$.

whether MDL-811 could regulate EZH2 acetylation under our experimental conditions, we assessed the levels of acetylated EZH2 by immunoprecipitation. RAW264.7 cells were treated with MDL-811, and EZH2 was immunoprecipitated using anti-EZH2. After that, we used an antibody specific for acetylated lysine (anti-Ac-K) to examine acetylation of EZH2 by

immunoblots. The acetylation of EZH2 was decreased in cells treated with MDL-811 (Fig. 4A and Supporting Information Fig. S4A), which was blocked by *Sirt6* gene silencing (Fig. 4B and Fig. S4B). To determine whether EZH2 was deacetylated by SIRT6, we also investigated the interaction between SIRT6 and EZH2. The results of the protein interaction analysis (Fig. 4A

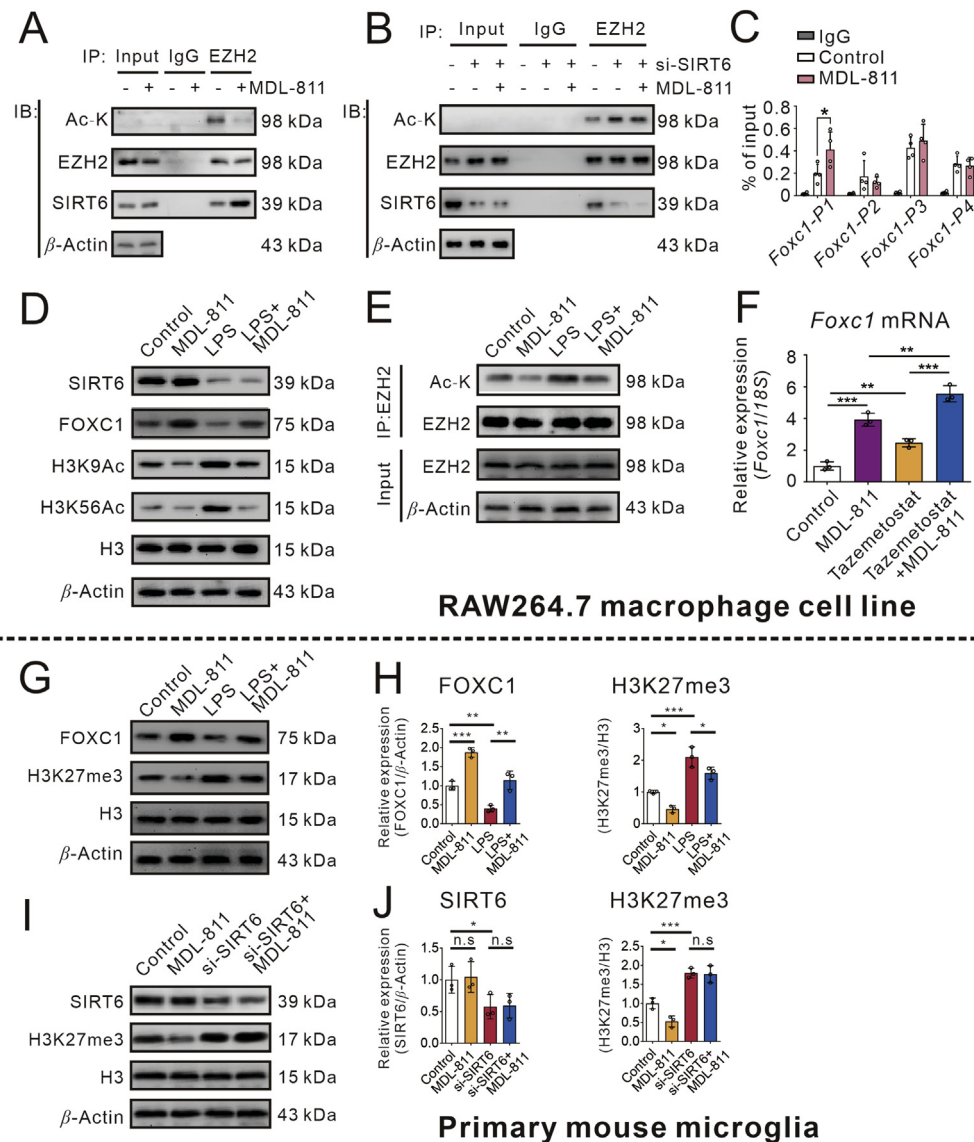


Figure 4 SIRT6-promoted EZH2 deacetylation and FOXC1 expression are central to the anti-inflammation of MDL-811. (A) Acetylated EZH2 levels in RAW264.7 cells incubated with MDL-811 or DMSO were measured by immunoprecipitation with anti-EZH2 and immunoblotting with anti-Ac-K. Interactions between EZH2 and SIRT6 were evaluated by co-immunoprecipitation. IgG is the negative control and β -actin is the input loading control. Data are representative of three independent experiments. (B) Acetylated EZH2 levels after silencing SIRT6 in RAW264.7 cells incubated with MDL-811 or DMSO were measured by immunoprecipitation with anti-EZH2 and immunoblotting with anti-Ac-K. Interactions between EZH2 and SIRT6 were evaluated by co-immunoprecipitation. IgG is the negative control and β -actin is the input loading control. Data are representative of three independent experiments. (C) ChIP assays in RAW264.7 cells incubated with MDL-811 or DMSO. Chromatin was immunoprecipitated with anti-EZH2 or anti-IgG, and the amounts of precipitated *Foxc1* promoter fragments were determined by q-PCR using the specific primer sets ($n = 3$). Data are representative of three independent experiments. Results are expressed as mean \pm SEM; $*P < 0.05$. (D) Western blot analysis on expression of FOXC1, SIRT6, H3K9Ac, and H3K56Ac in RAW264.7 cells incubated with 5 μ mol/L of MDL-811 in normal condition or LPS-stimulated condition. H3 is the internal control and β -actin is the loading control. Data are representative of three independent experiments. (E) Acetylated EZH2 levels in RAW264.7 cells incubated with 5 μ mol/L of MDL-811 in normal condition or LPS-stimulated condition measured by immunoprecipitation with anti-EZH2 and immunoblotting with anti-Ac-K. (F) Effects of EZH2 inhibitor tazemetostat on mRNA expression of *Foxc1* in RAW264.7 cells ($n = 3$). Results were normalized to 18S rRNA. Data are representative of three independent experiments. Results are expressed as mean \pm SEM; $**P < 0.01$, $***P < 0.001$. (G) and (H) Western blot analysis on expression of FOXC1 and H3K27me3 in primary mouse microglia incubated with 1 μ mol/L of MDL-811 in normal condition or LPS-stimulated condition. H3 is the internal control and β -actin is the loading control. Data are representative of three independent experiments. Results are expressed as mean \pm SEM; n.s.: not significant, $*P < 0.05$, $**P < 0.01$, $***P < 0.001$. (I) and (J) The H3K27me3 levels after silencing SIRT6 in primary mouse microglia incubated with MDL-811 or DMSO were measured by Western blot. H3 is the internal control and β -actin is the loading control. Data are representative of three independent experiments. Results are expressed as mean \pm SEM; n.s.: not significant, $*P < 0.05$, $**P < 0.01$.

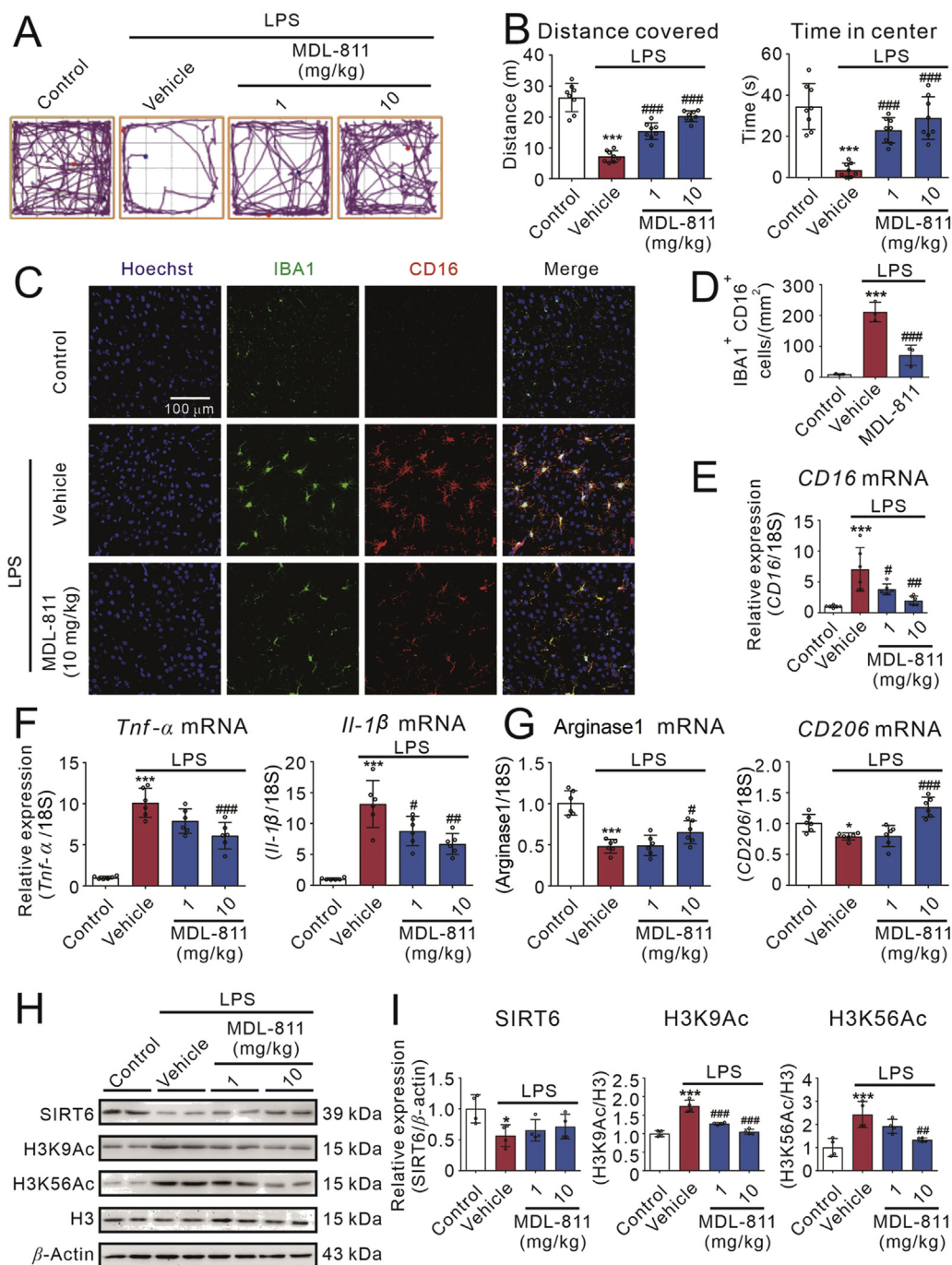


Figure 5 SIRT6 activator MDL-811 effectively ameliorates brain inflammation in LPS-induced neuroinflammatory mice model. (A) and (B) Track plots, distance covered and time in the center zone of the open field test. Mice were administrated with MDL-811 (1 or 10 mg/kg) or corresponding vehicle (1% DMSO in normal saline) followed by administration of LPS (0.33 mg/kg) or normal saline ($n = 8$). Data are representative of two independent experiments. (C) Representative double-staining immunofluorescence of IBA1 (green) and CD16 (red) in the cortex of the brain sections. (D) Quantification of IBA1⁺ CD16⁺ cells in the cortex of the brains ($n = 3$). (E) and (F) Treatment of MDL-811 dose-dependently inhibited the elevation of LPS-induced pro-inflammatory factor genes (*CD16*, *Tnf-α* and *Il-1β*) expressions in the cerebral cortex of the brain of mice ($n = 6$). Results were normalized to 18S rRNA. Data are representative of three independent experiments. (G) Treatment of MDL-811 significantly elevated the anti-inflammatory factor genes (arginase1, *CD206*) expressions in the cerebral cortex of the brain of LPS-induced neuroinflammatory mice ($n = 6$). Results were normalized to 18S rRNA. Data are representative of three independent experiments. (H) and (I) Western blot analysis on expression of SIRT6, H3K9Ac and H3K56Ac in the cerebral cortex of the brain of mice at 3 h after treatment of LPS ($n = 4$). H3 is the internal control and β-actin is the loading control. Data are representative of three independent experiments. Results in this figure are expressed as mean ± SEM; * $P < 0.05$, ** $P < 0.01$, *** $P < 0.001$ versus the sham group; # $P < 0.05$, ## $P < 0.01$, ### $P < 0.001$ versus the vehicle group.

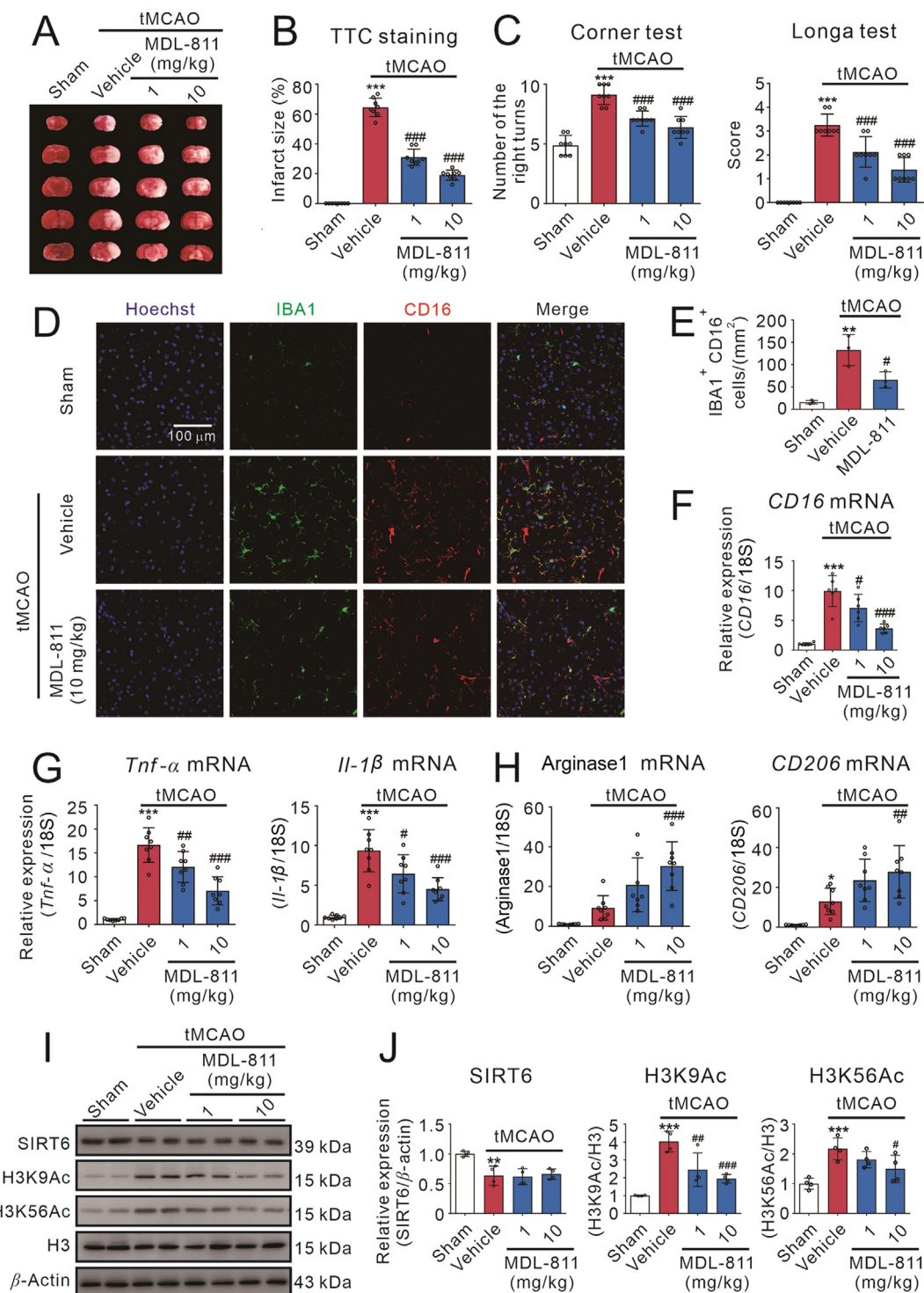


Figure 6 SIRT6 activator MDL-811 ameliorates brain ischemic injury and neuroinflammation in tMCAO mice. MDL-811 (1 or 10 mg/kg) reduced brain infarct size (A and B) and ameliorated neurological deficits evaluated by Longa test and corner test (C) after mice were subjected to tMCAO for 72 h ($n = 8$). Data are representative of two independent experiments. (D) Representative double-staining immunofluorescence of IBA1 (green) and CD16 (red) in the peri-infarct areas of the brain sections. (E) Quantification of IBA1⁺ CD16⁺ cells in the peri-infarct areas of the ischemic brains ($n = 3$). MDL-811 significantly reduced the mRNA levels of pro-inflammatory factors, including *CD16* (F) *Tnf-α* and *Il-1β* (G), and enhanced anti-inflammatory factors mRNA expressions, including arginase1 and *CD206* (H) in the cortex of peri-infarct region at 72 h after mice were subjected to tMCAO ($n = 8$). Results were normalized to 18S rRNA. Data are representative of three independent experiments. Western blot analysis (I and J) on the expression of SIRT6, H3K9Ac and H3K56Ac in the peri-infarct cerebral cortex region of mice at 72 h post tMCAO treated with or without MDL-811 ($n = 4$). H3 is the internal control and β-actin is the loading control. Data are representative of three independent experiments. Results in this figure are expressed as mean ± SEM; * $P < 0.05$, ** $P < 0.01$, *** $P < 0.001$ versus the sham group; # $P < 0.05$, ## $P < 0.01$, ### $P < 0.001$ versus the vehicle group.

and Fig. S4A) indicate that there was a direct interaction between SIRT6 and EZH2 (Fig. 4A and Fig. S4A). However, these interactions were alleviated by SIRT6 knockdown (Fig. 4B and Fig. S4B), indicating that EZH2 may serve as a direct substrate of SIRT6.

We next examined the binding of EZH2 at different regions of *Foxc1* promoter in RAW264.7 cells by ChIP assays. The results showed that the binding of EZH2 at transcriptional start P1 region of *Foxc1* promoter was apparently increased after treated with MDL-811 (Fig. 4C). However, other regions of *Foxc1* promoter were not changed significantly. These data showed that MDL-811 could upregulate *Foxc1* gene expression and promote the EZH2 binding to its promoter.

To confirm MDL-811 exhibits anti-inflammatory effects via SIRT6/EZH2/FOXC1 pathway, we examined the SIRT6, H3K9Ac, H3K56Ac, EZH2Ac and FOXC1 proteins expression in LPS-stimulated RAW264.7 cells. As shown in Fig. 4D and E, Fig. S4C and S4D, MDL-811 treatment significantly decreased the H3K9Ac, H3K56Ac and EZH2Ac protein levels, but increased the FOXC1 protein expression levels in RAW264.7 cells incubated with or without LPS.

Tazemetostat (EPZ-6438) is a potent EZH2 inhibitor which has been conducted in clinical study⁴¹. To investigate whether it affects the target gene *Foxc1* expression, RAW264.7 cells were treated with 5 $\mu\text{mol/L}$ of tazemetostat for 72 h followed with MDL-811 treatment for another 2 h. Total RNAs were extracted and *Foxc1* mRNA expression was evaluated by qPCR. As shown in Fig. 4F, MDL-811 or tazemetostat elevated the gene expression of *Foxc1*, and combination of MDL-811 and tazemetostat treatment exhibited an additive effect, which indicates that either EZH2 inhibition by its inhibitor tazemetostat or its deacetylation by MDL-811 could promote the expression of its target gene *Foxc1*.

In addition, the above results were validated in primary mouse microglia. Due to the difficulty in isolating enough primary microglia cells for immunoprecipitation assay, we detected the trimethylation of H3K27 (H3K27me3) expression levels indirectly, which is the EZH2 substrate. The trimethylation of H3K27 was decreased in cells treated with MDL-811 (Fig. 4G and Fig. S4E), which was blocked by *Sirt6* gene silencing (Fig. 4H and Fig. S4F). As show in Fig. 4G and S4E, FOXC1 expression was downregulated after treated with LPS while MDL-811 treatment enhanced FOXC1 expression in LPS-incubated primary mouse microglia. As a result, anti-inflammatory effects of MDL-811 were mediated by activation of SIRT6 which leads to deacetylation of EZH2 followed by FOXC1 upregulation in both RAW264.7 cells and primary mouse microglia.

3.5. MDL-811 treatment improves neurobehavioral deficits in LPS-induced neuroinflammatory mice

Given that SIRT6 activator MDL-811 has a potent anti-inflammatory effect *in vitro*, we want to confirm whether activating SIRT6 with MDL-811 suppresses neuroinflammation in mice. Thus, we established the LPS-induced neuroinflammatory mice model to evaluate the anti-inflammatory effects of MDL-811 *in vivo*. In the open field test (Fig. 5A), MDL-811 (1 or 10 mg/kg) markedly reversed the LPS-induced downregulation of total distance covered (Fig. 5B), time in the central zone (Fig. 5B), mean speed (Supporting Information Fig. S5A), line crossings (Fig. S5A) and distance in the corner zone (Fig. S5A), indicating

that MDL-811 ameliorates the sickness behaviors in LPS-induced neuroinflammatory mice.

Neuroinflammation induced by LPS is partially regulated by microglia. Here, we tested whether MDL-811 could regulate microglia/macrophage activation after the LPS challenge. Consistent with *in vitro* studies, ionized calcium-binding adapter molecule 1 (IBA1, a marker of microglia/macrophage) immunostaining demonstrated that MDL-811 attenuated the proliferation of microglia/macrophages in the brains at 3 h after LPS challenge (Fig. 5C and D). Additionally, we found that MDL-811 treatment significantly decreased pro-inflammatory microglia/macrophages (Fig. 5C and D), as found by the decrease in number of CD16⁺ IBA1⁺ cells. These data suggest that MDL-811 could ameliorate the LPS-induced neuroinflammation in mice.

Moreover, we detected the TNF- α protein level in the mice serum after the open field test. Interestingly, MDL-811 (10 mg/kg) markedly reduced the LPS-induced TNF- α release (Fig. S5B). We also detected the gene expression of pro-inflammatory and anti-inflammatory factors in the cerebral cortex of mice after the open field test. Compared with LPS group, MDL-811 significantly reduced the gene expression of pro-inflammatory factors (Fig. 5E and F and Fig. S5C). Conversely, MDL-811 significantly elevated the gene expression of anti-inflammatory factors (Fig. 5G and Fig. S5C).

Furthermore, we investigated whether SIRT6 is involved in the anti-inflammatory effects of MDL-811 in LPS-induced neuroinflammatory mice model. Our results shown that it was observed that SIRT6 was decreased and its substrate H3K9Ac and H3K56Ac were both increased in cerebral cortex of mice after administrated LPS (Fig. 5H and I). Mice treated with 1 or 10 mg/kg of MDL-811 before administrated with LPS showed no effect on expression of SIRT6, but the acetylation levels of H3K9 and H3K56 were significantly decreased by MDL-811 administration dose-dependently. On the contrary, MDL-811 hardly affected H3K14Ac, a substrate of SIRT1 (Fig. S5D). Therefore, these results suggest that MDL-811 activates SIRT6 to reduce neuroinflammation and ameliorate sickness behaviors in LPS-induced neuroinflammatory mice.

3.6. MDL-811 treatment reduces brain damage and improves neurobehavioral deficits in mice subjected to tMCAO

Massive inflammation is surrounded with injured area of stroke patients that magnifies the neuronal damage⁴². To evaluate the neuroprotective effects of MDL-811 in mice subjected to tMCAO, the infarct size was assessed. The TTC staining results (Fig. 6A and B) show that MDL-811 significantly reduced the infarct size measured 3 days after tMCAO compared with the vehicle group. To examine the effect of MDL-811 on the neurological deficits, we performed the modified Longa test and the corner test (Fig. 6C and Supporting Information Table S3). The results of the modified Longa test show that MDL-811 group had a lower score than the vehicle group. Plus, the results of the corner test show that the number of the MDL-811 group turning to right was lower than that of the vehicle group.

Microglia/macrophage activation with continuous emission of inflammatory mediators is known to impair neurological functions after ischemic stroke⁴². Here, we found the number of cells positive for the general marker IBA1 and the phagocytosis marker CD16 were remarkably elevated in tMCAO mice (Fig. 6D and E). Microglia/macrophages in the peri-infarct area of ischemic brains were remarkably activated 3 days after tMCAO, characterized by

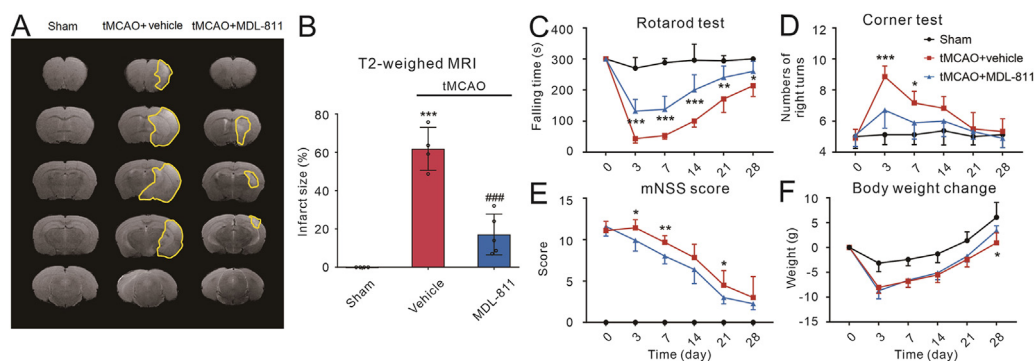


Figure 7 MDL-811 promotes long-term functional recovery in mice subjected to tMCAO. (A) and (B) Representative T2-weighted MRI of mice on the day 14 post tMCAO. Infarct volumes were decreased in MDL-811 treatment (10 mg/kg) group compared with vehicle group, as demonstrated by MRI ($n = 4-5$). Results are expressed as mean \pm SEM; $***P < 0.001$ versus sham group; $####P < 0.001$ versus the vehicle group. (C)–(F) MDL-811 treatment significantly promoted sensorimotor function of mice subjected to tMCAO as evaluated by the rotarod test, corner test and mNSS test, and change of the body weight after tMCAO ($n = 6-8$). Results are expressed as mean \pm SEM; $*P < 0.05$, $**P < 0.01$, $***P < 0.001$ versus vehicle group.

hypertrophic morphology, with thickened and retracted processes. In contrast, MDL-811 (10 mg/kg)-treated mice showed fewer IBA1⁺ CD16⁺ microglia/macrophages displaying smaller cell bodies and thinner processes (Fig. 6D and E). These data suggest that the brain damage and neurological deficits of mice after stroke were ameliorated by MDL-811 treatment.

Furthermore, we examined the gene expression of pro-inflammatory and anti-inflammatory factors in the peri-infarct zone of brain cortex on the third day following ischemia/reperfusion. MDL-811 significantly reduced the gene expression of pro-inflammatory factors compared with the vehicle group (Fig. 6F and G and Fig. S6B). Conversely, MDL-811 significantly enhanced the gene expression of anti-inflammatory factors (Fig. 6H and Fig. S6B) compared with the vehicle group.

In the meantime, we further investigated whether SIRT6 is involved in the anti-ischemic effect of MDL-811. It was observed that SIRT6 was decreased and its substrates H3K9Ac and H3K56Ac were increased in the peri-infarct of cerebral cortex of mice with tMCAO (Fig. 6I and J). After treated with 1 or 10 mg/kg of MDL-811, although expression of SIRT6 was not changed, the acetylation levels of H3K9 and H3K56 were significantly decreased in a dose-dependent manner. On the contrary, MDL-811 hardly affected H3K14Ac, a substrate of SIRT1 (Fig. S6C). Therefore, these data indicate that MDL-811 ameliorates neuroinflammation and brain ischemic injury through activating SIRT6 in mice subjected to tMCAO.

3.7. MDL-811 promotes long-term functional recovery in mice after tMCAO

To assess the effect of MDL-811 on reducing infarction and ameliorating neurobehavioral deficits after I/R injury in chronic phase, body weight changes, and neurological behaviors were recorded on the Days 0, 3, 7, 14, 21 and 28 post tMCAO. Also, infarct volume on the Day 14 was detected by brain MRI scanning. Rotarod test, corner test and mNSS test were performed to test the sensorimotor function of mice subjected to tMCAO. From the MRI scanning results, we found MDL-811-treated mice showed a smaller infarct volume than that of the vehicle group on the Day 14 after tMCAO (Fig. 7A and B). We found mice subjected to tMCAO showed severe impairment in the rotarod test.

Interestingly, the falling time of mice treated with MDL-811 in the rotarod test was significantly longer than that of the vehicle group after tMCAO (Fig. 7C). In the corner test, mice treated with MDL-811 showed a lower number of right turns on Days 3–7 after tMCAO (Fig. 7D). Moreover, compared with the vehicle-treated mice, MDL-811-treated mice had lower scores in the mNSS test (Fig. 7E and Supporting Information Table S4), suggesting MDL-811-treated mice performed a favorable outcome after I/R injury. Body weight loss was an important index of mice physical conditions in this study. All mice's body weight was decreased on the Day 3 after tMCAO, while those administrated MDL-811 regained body weight faster than vehicle group (Fig. 7F). Taken together, these results indicate that MDL-811 significantly promoted long-term functional recovery and improved long-term neurobehavioral deficits in mice subjected to tMCAO.

3.8. SIRT6/EZH2/FOXC1 pathway is critical for MDL-811 anti-neuroinflammation and anti-ischemia in vivo

We subsequently examined the involvement of SIRT6/EZH2/FOXC1 axis in LPS-induced neuroinflammation model and ischemic stroke model in mice. Similar to the results *in vitro*, EZH2 acetylation and H3K27me3 expression were significantly upregulated, and FOXC1 expression was downregulated in cerebral cortex of the brain of mice treated with LPS, which could be reversed by MDL-811 (Fig. 8A–C). In addition, the EZH2 acetylation and H3K27me3 expression levels were increased, and FOXC1 expression was decreased in the peri-infarct of cerebral cortex of the brain of mice subjected to tMCAO, which could be reversed by MDL-811 (Fig. 8D–F). These results suggest that the SIRT6/EZH2/FOXC1 pathway may be involved in the beneficial effects of MDL-811 in brain inflammatory mice and ischemic stroke mice.

3.9. MDL-811 inhibits LPS-induced inflammatory response in primary human monocytes of patients with ischemic stroke

To further substantiate the translational relevance of the data we gained from cell models and animal models, we performed LPS-induced inflammation model in peripheral blood monocytes isolated from brain ischemic stroke patients. A total of 7 ischemic

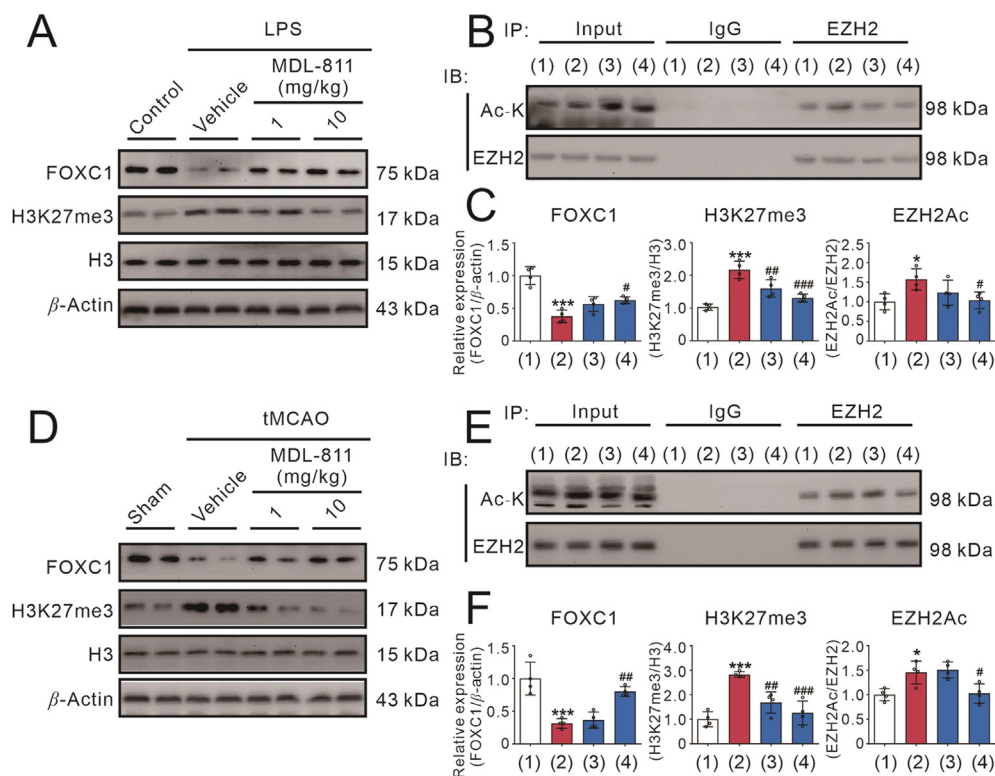


Figure 8 The SIRT6-mediated EZH2/FOXC1 pathway is critical for the beneficial effects of MDL-811 in LPS-induced neuroinflammatory mice model and brain ischemic stroke mice model. (A) Western blot analysis on the protein expression of FOXC1 and H3K27me3 in the cerebral cortex region of the brain of mice at 3 h after treatment of LPS ($n = 4$). Results were normalized to H3 or β -actin. Data are representative of three independent experiments. (B) Acetylated EZH2 levels in the cerebral cortex region of mice at 3 h after treatment of LPS ($n = 4$). IgG is the negative control and β -actin is the input loading control. Data are representative of three independent experiments. (1) Control; (2) LPS+vehicle; (3) LPS+MDL-811 (1 mg/kg); (4) LPS+MDL-811 (10 mg/kg). (C) Statistical analysis of the immunoblots in (A) and (B). Results are expressed as mean \pm SEM; * $P < 0.05$, *** $P < 0.001$ versus control group; # $P < 0.05$, ### $P < 0.01$, #### $P < 0.001$ versus vehicle group. (D) Western blot analysis on the protein expression of FOXC1 and H3K27me3 in the peri-infarct cerebral cortex region of the brain of mice at 72 h post tMCAO treated with MDL-811 ($n = 4$). Data are representative of three independent experiments. (E) Acetylated EZH2 levels in the peri-infarct cerebral cortex region of mice at 72 h post tMCAO treated with MDL-811 ($n = 4$). IgG is the negative control and β -actin is the input loading control. Data are representative of three independent experiments. (1) Sham; (2) tMCAO+vehicle; (3) tMCAO+MDL-811 (1 mg/kg); (4) tMCAO+MDL-811 (10 mg/kg). (F) Statistical analysis of the immunoblots in (D) and (E). Results are expressed as mean \pm SEM; * $P < 0.05$, *** $P < 0.001$ versus sham group; # $P < 0.05$, ### $P < 0.01$, #### $P < 0.001$ versus the vehicle group.

stroke patients and 7 healthy controls were included in this experiment. After treated with MDL-811 followed by treated with LPS, *SIRT6* gene expression was not significantly changed. However, we found various pro-inflammatory factors were descended with the treatment of MDL-811, including *TNF- α* , *IL-1 β* , and *NOS2* (Fig. 9A). We also monitored SIRT6 activity, indicated by H3K9Ac and H3K56Ac, together with the involvement of FOXC1/EZH2 signaling pathway using Western blots. Our data reveal that MDL-811 increased SIRT6 activity by deacetylating H3K9 and H3K56. Moreover, it inhibited the activity of EZH2 indicated by decreasing trimethylation of H3K27, and it promoted expression of FOXC1 in human monocytes of patients with stroke (Fig. 9B and Supporting Information Fig. S7).

Finally, we tried to reveal the correlation between *SIRT6* expression levels and anti-inflammatory effect of MDL-811 in primary human monocytes. Interestingly, we found that *SIRT6* mRNA in stroke patients' blood was significantly lower than that in healthy controls (Fig. 9C). Furthermore, we found a positive correlation between *SIRT6* gene expression and *TNF- α* inhibition

rate (Fig. 9D), indicating that MDL-811 treatment could activate *SIRT6* to inhibit inflammatory response in stroke patients and would show more beneficial effects in stroke patients with higher expression of *SIRT6*.

4. Discussion

Growing evidence has demonstrated that regulating microglia activation contributes to the outcome after ischemic stroke⁴³. Microglial activation is a vital process in producing and releasing inflammatory mediators during the progression of ischemic stroke⁴⁴. Thus, primary mouse microglia cells were commonly used in *in vitro* inflammatory models. In order to broaden our horizon of the molecular mechanism underlying microglia activation and phenotype transition to identify novel therapeutic targets for neuroinflammation, we previously investigated the role of various inflammatory genes in the setting of ischemic stroke. Among sirtuins, SIRT6 has also been implicated to produce

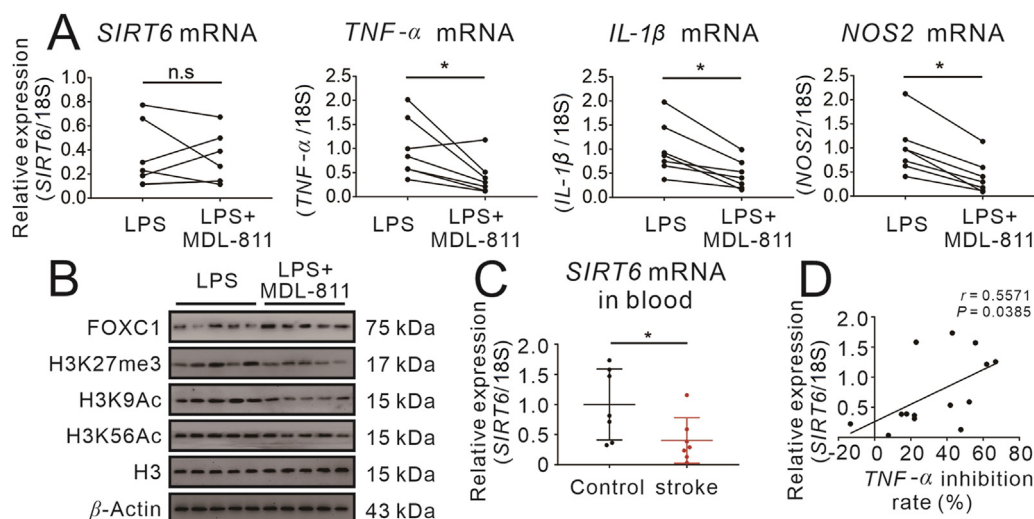


Figure 9 SIRT6 activator MDL-811 inhibits inflammatory response in monocytes of patients with ischemic stroke. (A) MDL-811 significantly reduced the mRNA expression of proinflammatory genes (*TNF-α*, *IL-1β* and *NOS2*) but had no effect on *SIRT6* mRNA expression in monocytes isolated from stroke patients. Cells were incubated with 1 $\mu\text{mol/L}$ of MDL-811 for 2 h and then stimulated with 50 ng/mL LPS for another 2 h ($n = 7$). Results were normalized to 18S rRNA. n.s.: no significant, $*P < 0.05$. (B) Western blot analysis on the protein expression of FOXC1, H3K9Ac, H3K56Ac and H3K27me3 in monocytes from stroke patients incubated with 50 ng/mL LPS and 1 $\mu\text{mol/L}$ of MDL-811 ($n = 5$). H3 is the internal control and β -actin is the loading control. Data are representative of three independent experiments. The experiments were repeated three times on different days. (C) *SIRT6* mRNA expression in blood is decreased in ischemic stroke patients as compared to healthy controls ($n = 7$). Results were normalized to 18S rRNA. The experiments were repeated three times on different days; $*P < 0.05$. (D) There is a linear correlation between *SIRT6* transcript levels in blood and anti-inflammatory effect of MDL-811 in monocytes of ischemic stroke patients and healthy controls ($n = 14$).

beneficial effects in ischemic stroke in recent studies both *in vitro* and *in vivo*. Endothelial SIRT6 has been reported to blunt stroke size and neurological deficit through AKT signaling pathway⁴⁵ and neuronal SIRT6 has been reported to protect the brain from ischemia/reperfusion injury through deacetylation of NRF2¹⁸. In addition, a few studies have demonstrated that SIRT6 plays an essential role in cells exposed to OGD/R^{21,46}. High expression of SIRT6 has been found in primary neuronal cells, and the reduced expression of SIRT6 enhances the OGD-induced release of inflammatory factor HMGB1. All these studies suggest that SIRT6 may serve as a promising target, and pharmacological activation of SIRT6 may prove the potential for novel therapeutic intervention for inflammation after cerebral ischemia. However, the biofunction and exact regulatory mechanism of microglial SIRT6 in neuroinflammation and ischemic stroke are still elusive. Our findings suggest that microglial SIRT6 might participate in the regulation of pathology of ischemic stroke and SIRT6 activators might be able to exhibit anti-neuroinflammatory and neuroprotective effects in ischemic stroke. Here, we investigated, for the first time, the pharmacological action of a novel SIRT6 activator MDL-811 in neuroinflammation and ischemic stroke using animal models, primary mouse microglia and primary human monocytes models.

In this study, we demonstrate for the first time that small-molecule SIRT6 activator MDL-811 attenuated brain tissue damage and improved outcomes after ischemia/reperfusion cerebral injury or LPS-induced neuroinflammation in good accordance of previous studies from other groups^{18,21,45}. Several results substantiate our conclusions: (I) SIRT6 activity is downregulated in LPS/OGD-induced microglia/macrophage/monocyte activation, LPS-induced neuroinflammatory mice and brain ischemic stroke mice, while specific SIRT6 activator MDL-811 could ameliorate neuroinflammation and neurologic deficits by SIRT6 activation;

(II) SIRT6 silencing abolishes the anti-inflammatory effects of MDL-811 in microglia/macrophages; (III) SIRT6 activation by MDL-811 deacetylated EZH2 and promoted the expression of FOXC1 to perform its anti-inflammatory effects; (IV) SIRT6 activator MDL-811 ameliorates brain ischemic injury of mice and improves stroke outcomes through inhibiting microglia/macrophage activation; and (V) SIRT6 activation by MDL-811 exhibits anti-inflammatory effects in human monocytes from stroke patients. Taken together, our results indicated that SIRT6 activator MDL-811 might ameliorate cerebral ischemia–reperfusion injury and neuroinflammation after tMCAO *via* at least partly the SIRT6/EZH2/FOXC1 pathway.

In our experiments, microglial SIRT6 activation is associated with OGD injury and brain ischemic injury, complementing what has been already shown in neuronal cells¹⁸ and endothelial cells⁴⁵ by other groups. Similar to previous findings by Lee et al.²¹, we detected decreased SIRT6 levels after tMCAO. Furthermore, our findings are reinforced by the observation that SIRT6 activator MDL-811 can attenuate brain injury after cerebral ischemia/reperfusion through reducing neuroinflammation partly by microglial SIRT6 activation. These results are consistent with the previous findings that SIRT6 overexpression attenuates cerebral I/R-induced brain tissue damage and neurological deficits in mice^{11,18,45}. It is conceivable that overexpression of microglial SIRT6 might also have a similar effect as MDL-811 and overexpression of SIRT6 may further potentiate the effects of MDL-811.

Neuroinflammation associates to worsen clinical outcomes after ischemic stroke⁴⁷. In addition, neuroinflammation after ischemia is involved with microglia/macrophage activation. Work by Jiang et al.⁴⁸ demonstrated that SIRT6 played an anti-inflammatory role by regulating TNF- α secretion in mouse embryonic fibroblast cells. TNF- α is a potent proinflammatory

cytokine to activate NF- κ B. Besides tMCAO model, peripheral LPS challenge can also lead to neuroinflammation in mice⁴⁹. In LPS-induced microglia/macrophage activation model and neuro-inflammatory mice model, SIRT6 activator MDL-811 significantly reduced microglia/macrophage activation and sickness behaviors accompanied by downregulation of pro-inflammatory factors and upregulation of anti-inflammatory mediators, which were associated with SIRT6 activation and could be abolished by silencing SIRT6. Also, we noticed that MDL-811 reduced LPS-induced TNF- α release in the serum, suggesting MDL-811 may also reduce systemic inflammation besides neuroinflammation. In this study, intraperitoneal injection of LPS may cause inflammatory response in other organs such as lung, liver, etc. It is possible that the improved performance by MDL-811 may be due to the reduction of both systemic inflammation and neuroinflammation. Furthermore, MDL-811 could also reduce LPS-induced inflammatory response in human monocytes from stroke patients, which might provide SIRT6 as a potential target for brain ischemic stroke and other inflammatory diseases in clinical research.

FOXC1 is one of the forkhead box transcription factors, which plays an essential role in various diseases such as colorectal cancer⁵⁰, cerebral small-vessel diseases⁵¹ and lymphatic-associated diseases⁵². FOXC1 regulates the RAS/ERK signaling cascade⁵², which is closely related to inflammation⁵³. Overexpression of FOXC1 might attenuate inflammatory responses through intervening in the crosstalk between autophagy and ERK/MAPK pathway, and might be a potential target treating inflammation-related diseases. Regarding the mechanisms responsible for the anti-inflammatory effects of MDL-811, we demonstrated that MDL-811 treatment upregulated FOXC1 expression time- and concentration-dependently in macrophages and microglia while the anti-inflammatory effects were eliminated by silencing FOXC1 in both cells. This finding was consistent with the previous study that FOXC1 overexpression attenuated inflammation, oxidative stress and apoptosis in chronic obstructive pulmonary disease⁵⁴. Moreover, Du et al.²⁸ indicated that post-translational modifications, including methylation and acetylation, played a crucial role in FOXC1 expression. They also validated that FOXC1 was a target gene of the polycomb group protein family, among which EZH2 played a dominant role in regulating FOXC1 expression. In the present study, we found that the deacetylation of EZH2 regulated by MDL-811 promoted its binding to the promoter of FOXC1.

Acetylation is a dynamic process and can be deacetylated by relevant deacetylase⁵⁵. Emerging studies revealed that acetylation, including histone and non-histone acetylation, is an important form of post-translational modifications^{56,57}. Acetylation of non-histone proteins plays a crucial role for silencing target genes and regulates diverse biological functions including ischemic stroke³⁵. EZH2 is a crucial epigenetic regulator that catalyzes the trimethylation of H3K27 and is modulated by post-translational modifications⁵⁸. It is involved in large amounts of cellular processes such as proliferation⁵⁹, invasion⁶⁰, self-renewal⁶¹, inflammation⁶² and microglia/macrophage activation⁶³. Interestingly, SIRT1, one of the HDACs, can deacetylate EZH2 and affect its phosphorylation, stability and capacity, correlated with repressing the expression of target genes²⁹. We speculated that SIRT6, another HDAC expressed in nucleus, might have similar deacetylation effects. In our study, we found that EZH2 could be deacetylated by SIRT6 in microglia/macrophages and deacetylation of EZH2 promoted expression of FOXC1 by increasing binding capacity

to its promoters in both *in vitro* and *in vivo* studies. MDL-811, a novel SIRT6 activator, participates in the anti-inflammation process through EZH2/FOXC1 signaling pathway as a valuable pharmacological probe, indicating that SIRT6/EZH2/FOXC1 axis plays an important regulatory role in anti-inflammation *in vitro* and anti-neuroinflammation *in vivo*.

To strengthen the significance of our pre-clinical research, we further investigated the anti-inflammatory effect of MDL-811 in primary human monocytes. We performed LPS-induced inflammatory response model in peripheral blood monocytes isolated from stroke patients. Interestingly, we found that cells from different individuals showed different responses to MDL-811. In the meantime, we detected the *SIRT6* gene expression in the whole blood of the subjects. MDL-811 remarkably reduced pro-inflammatory factors expression induced by LPS. Moreover, we notified that *SIRT6* mRNA levels were decreased in the blood of ischemic stroke patients, which is similar to that in previously reported animal studies^{18,64}, showing that *SIRT6* gene expression is increased in ischemic stroke patients with short-term neurological improvement and correlates with stroke outcome. Interestingly, we found a positive correlation between *SIRT6* gene expression in monocytes and TNF- α inhibition rate by MDL-811, suggesting that *SIRT6* mRNA levels are strongly correlated with the anti-inflammatory effect of MDL-811. In a word, the translational study reveals that targeting SIRT6 by activators could be a potential therapeutic strategy for ischemic stroke in future clinical research.

There are still a few limitations to the present study. Firstly, although we found that SIRT6 played an important role in LPS-induced microglial activation *in vitro* and SIRT6 activator MDL-811 ameliorated the brain injury and neuroinflammation *in vivo*, other cells besides microglia contributing to the results with SIRT6 activation cannot be excluded. The microglial SIRT6 knockout mice could be used to demonstrate whether MDL-811 targets microglial SIRT6 to show beneficial effects *in vivo*. Secondly, *Foxc1* gene may not be the only target of SIRT6 activator MDL-811. Whether MDL-811 participates in other signaling pathways to exert anti-ischemic and anti-inflammatory effects should be further studied. Thirdly, the deacetylation site of EZH2 is still unknown. The site-directed amino acid mutation technology could be used to confirm the deacetylation site of EZH2 and the specific anti-neuroinflammatory effects. Finally, considering the difficulty in collecting microglia in human, we chose monocytes in blood as surrogate cells to validate the anti-inflammatory effects of MDL-811 in stroke patients *in vitro*. We still have a limited understanding of the functions of microglial SIRT6 in ischemic stroke, and the combination of pharmacological modulation and genetics intervention is indeed needed for detailed elucidation of its role.

5. Conclusions

In conclusion, our findings in this study indicate that SIRT6 activator MDL-811 exerts favorable anti-neuroinflammation and neuroprotective effects in cerebral ischemia/reperfusion injury by SIRT6 activation. Mechanistically, MDL-811 modulates neuroinflammation through SIRT6/EZH2/FOXC1 signaling pathway. Data we acquired in this study might facilitate the validation of microglial SIRT6 as a novel therapeutic target and the potential

clinical use of SIRT6 activator MDL-811 for treating ischemic stroke in the near future.

Acknowledgments

This work was supported by the National Natural Science Foundation of China (81973512, 81925034, 81701235, and 81991514), Double First-Class Project of China Pharmaceutical University (CPU2018GY06 and CPU2018GY20, China), and the Fundamental Research Funds for the Central Universities (021414380446, China). This work was also supported by the Six Talent Peaks Project of Jiangsu Province (China) to Tao Pang.

Author contributions

Tao Pang, Jian Zhang, Cunjin Zhang, and Tailin He conceived the project and designed the studies. Tailin He, Jialin Shang and Tao Pang wrote the paper. Jian Zhang, Cunjin Zhang, and Luyong Zhang revised the manuscript. Jialin Shang and Yingyi Chen conducted compound synthesis, enzyme assay and molecular docking studies. Tailin He, Chenglong Gao, and Xin Guan conducted animal experiments. Tailin He, Chenglong Gao, Xin Guan, and Liwen Zhu performed the molecular biology and cell biology experiments.

Conflicts of interest

The authors declare that there are no competing interests.

Appendix A. Supporting information

Supporting data to this article can be found online at <https://doi.org/10.1016/j.apsb.2020.11.002>.

References

- Rolfs A, Fazekas F, Grittner U, Dichgans M, Martus P, Holzhausen M, et al. Acute cerebrovascular disease in the young: The stroke in young fabry patients study. *Stroke* 2013;**44**:340–9.
- Song J, Zhang W, Wang J, Yang H, Zhou Q, Wang H, et al. Inhibition of FOXO3a/BIM signaling pathway contributes to the protective effect of salvianolic acid A against cerebral ischemia/reperfusion injury. *Acta Pharm Sin B* 2019;**9**:505–15.
- Wardlaw JM, Murray V, Berge E, del Zoppo GJ. Thrombolysis for acute ischaemic stroke. *Cochrane Database Syst Rev* 2014;**2014**:Cd000213.
- Jin WN, Shi SX, Li Z, Li M, Wood K, Gonzales RJ, et al. Depletion of microglia exacerbates postischemic inflammation and brain injury. *J Cerebr Blood Flow Metabol* 2017;**37**:2224–36.
- Brown GC, Neher JJ. Microglial phagocytosis of live neurons. *Nat Rev Neurosci* 2014;**15**:209–16.
- Rahimifard M, Maqbool F, Moeini-Nodeh S, Niaz K, Abdollahi M, Braidy N, et al. Targeting the TLR4 signaling pathway by polyphenols: A novel therapeutic strategy for neuroinflammation. *Ageing Res Rev* 2017;**36**:11–9.
- Gomez Perdiguero E, Klapproth K, Schulz C, Busch K, Azzoni E, Crozet L, et al. Tissue-resident macrophages originate from yolk-sac-derived erythro-myeloid progenitors. *Nature* 2015;**518**:547–51.
- Wang J, Huang L, Cheng C, Li G, Xie J, Shen M, et al. Design, synthesis and biological evaluation of chalcone analogues with novel dual antioxidant mechanisms as potential anti-ischemic stroke agents. *Acta Pharm Sin B* 2019;**9**:335–50.
- Zhang W, Song JK, Zhang X, Zhou QM, He GR, Xu XN, et al. Salvianolic acid A attenuates ischemia reperfusion induced rat brain damage by protecting the blood brain barrier through MMP-9 inhibition and anti-inflammation. *Chin J Nat Med* 2018;**16**:184–93.
- Wang Y, Huang Y, Xu Y, Ruan W, Wang H, Zhang Y, et al. A dual AMPK/Nrf2 activator reduces brain inflammation after stroke by enhancing microglia M2 polarization. *Antioxidants Redox Signal* 2018;**28**:141–63.
- Watroba M, Dudek I, Skoda M, Stangret A, Rzodkiewicz P, Szukiewicz D. Sirtuins, epigenetics and longevity. *Ageing Res Rev* 2017;**40**:11–9.
- Liu J, Qian C, Cao X. Post-translational modification control of innate immunity. *Immunity* 2016;**45**:15–30.
- Zhu Y, Liu J, Park J, Rai P, Zhai RG. Subcellular compartmentalization of NAD⁺ and its role in cancer: A sereNADE of metabolic melodies. *Pharmacol Ther* 2019;**200**:27–41.
- Rizzo A, Iachettini S, Salvati E, Zizza P, Maresca C, D'Angelo C, et al. SIRT6 interacts with TRF2 and promotes its degradation in response to DNA damage. *Nucleic Acids Res* 2017;**45**:1820–34.
- Liu X, Cai S, Zhang C, Liu Z, Luo J, Xing B, et al. Deacetylation of NAT10 by Sirt1 promotes the transition from rRNA biogenesis to autophagy upon energy stress. *Nucleic Acids Res* 2018;**46**:9601–16.
- Gil R, Barth S, Kanfi Y, Cohen HY. SIRT6 exhibits nucleosome-dependent deacetylase activity. *Nucleic Acids Res* 2013;**41**:8537–45.
- Zhang P, Tu B, Wang H, Cao Z, Tang M, Zhang C, et al. Tumor suppressor p53 cooperates with SIRT6 to regulate gluconeogenesis by promoting FoxO1 nuclear exclusion. *Proc Natl Acad Sci U S A* 2014;**111**:10684–9.
- Zhang W, Wei R, Zhang L, Tan Y, Qian C. Sirtuin 6 protects the brain from cerebral ischemia/reperfusion injury through NRF2 activation. *Neuroscience* 2017;**366**:95–104.
- Zuo Y, Huang L, Enkhjargal B, Xu W, Umut O, Travis ZD, et al. Activation of retinoid X receptor by bexarotene attenuates neuroinflammation via PPARgamma/SIRT6/FoxO3a pathway after subarachnoid hemorrhage in rats. *J Neuroinflammation* 2019;**16**:47.
- Liu M, Liang K, Zhen J, Zhou M, Wang X, Wang Z, et al. Sirt6 deficiency exacerbates podocyte injury and proteinuria through targeting Notch signaling. *Nat Commun* 2017;**8**:413.
- Lee OH, Kim J, Kim JM, Lee H, Kim EH, Bae SK, et al. Decreased expression of sirtuin 6 is associated with release of high mobility group box-1 after cerebral ischemia. *Biochem Biophys Res Commun* 2013;**438**:388–94.
- Koo JH, Jang HY, Lee Y, Moon YJ, Bae EJ, Yun SK, et al. Myeloid cell-specific sirtuin 6 deficiency delays wound healing in mice by modulating inflammation and macrophage phenotypes. *Exp Mol Med* 2019;**51**:1–10.
- Kugel S, Mostoslavsky R. Chromatin and beyond: The multitasking roles for SIRT6. *Trends Biochem Sci* 2014;**39**:72–81.
- Peng SL. Forkhead transcription factors in chronic inflammation. *Int J Biochem Cell Biol* 2010;**42**:482–5.
- Berry FB, Skarie JM, Mirzayans F, Fortin Y, Hudson TJ, Raymond V, et al. FOXO1 is required for cell viability and resistance to oxidative stress in the eye through the transcriptional regulation of FOXO1A. *Hum Mol Genet* 2008;**17**:490–505.
- Ito YA, Goping IS, Berry F, Walter MA. Dysfunction of the stress-responsive FOXO1 transcription factor contributes to the earlier-onset glaucoma observed in Axenfeld-Rieger syndrome patients. *Cell Death Dis* 2014;**5**:e1069.
- Ray PS, Wang J, Qu Y, Sim MS, Shamonki J, Bagaria SP, et al. FOXO1 is a potential prognostic biomarker with functional significance in basal-like breast cancer. *Canc Res* 2010;**70**:3870–6.
- Du J, Li L, Ou Z, Kong C, Zhang Y, Dong Z, et al. FOXO1, a target of polycomb, inhibits metastasis of breast cancer cells. *Breast Canc Res Treat* 2012;**131**:65–73.
- Wan J, Zhan J, Li S, Ma J, Xu W, Liu C, et al. PCAF-primed EZH2 acetylation regulates its stability and promotes lung adenocarcinoma progression. *Nucleic Acids Res* 2015;**43**:3591–604.

30. Xu Y, Xu Y, Wang Y, Wang Y, He L, Jiang Z, et al. Telmisartan prevention of LPS-induced microglia activation involves M2 microglia polarization via CaMKK β -dependent AMPK activation. *Brain Behav Immun* 2015;**50**:298–313.
31. Huang Z, Zhao J, Deng W, Chen Y, Shang J, Song K, et al. Identification of a cellularly active SIRT6 allosteric activator. *Nat Chem Biol* 2018;**14**:1118–26.
32. Gao CL, Hou GG, Liu J, Ru T, Xu YZ, Zhao SY, et al. Synthesis and target identification of benzoxepane derivatives as potential anti-neuroinflammatory agents for ischemic stroke. *Angew Chem Int Ed Engl* 2020;**59**:2429–39.
33. Wang Z, Xu G, Gao Y, Zhan X, Qin N, Fu S, et al. Cardamonin from a medicinal herb protects against LPS-induced septic shock by suppressing NLRP3 inflammasome. *Acta Pharm Sin B* 2019;**9**:734–44.
34. Hu Y, Ruan W, Gao A, Zhou Y, Gao L, Xu M, et al. Synthesis and biological evaluation of novel 4,5-bisindolyl-1,2,4-triazol-3-ones as glycogen synthase kinase-3 β inhibitors and neuroprotective agents. *Pharmazie* 2017;**72**:707–13.
35. Wang Z, Leng Y, Wang J, Liao HM, Bergman J, Leeds P, et al. Tubastatin A, an HDAC6 inhibitor, alleviates stroke-induced brain infarction and functional deficits: Potential roles of alpha-tubulin acetylation and FGF-21 up-regulation. *Sci Rep* 2016;**6**:19626.
36. Chen J, Sanberg PR, Li Y, Wang L, Lu M, Willing AE, et al. Intravenous administration of human umbilical cord blood reduces behavioral deficits after stroke in rats. *Stroke* 2001;**32**:2682–8.
37. Kim WG, Mohny RP, Wilson B, Jeohn GH, Liu B, Hong JS. Regional difference in susceptibility to lipopolysaccharide-induced neurotoxicity in the rat brain: Role of microglia. *J Neurosci* 2000;**20**:6309–16.
38. Zeng Q, Ko CH, Siu WS, Li KK, Wong CW, Han XQ, et al. Inhibitory effect of different *Dendrobium* species on LPS-induced inflammation in macrophages via suppression of MAPK pathways. *Chin J Nat Med* 2018;**16**:481–9.
39. Zorrilla-Zubilete MA, Yeste A, Quintana FJ, Toiber D, Mostoslavsky R, Silberman DM. Epigenetic control of early neurodegenerative events in diabetic retinopathy by the histone deacetylase SIRT6. *J Neurochem* 2018;**144**:128–38.
40. Forma E, Jozwiak P, Ciesielski P, Zaczek A, Starska K, Brys M, et al. Impact of OGT deregulation on EZH2 target genes *FOXA1* and *FOXCl* expression in breast cancer cells. *PLoS One* 2018;**13**:e0198351.
41. Makita S, Tobinai K. Targeting EZH2 with tazemetostat. *Lancet Oncol* 2018;**19**:586–7.
42. Anrather J, Iadecola C. Inflammation and stroke: An overview. *Neurotherapeutics* 2016;**13**:661–70.
43. Chamorro A, Dirnagl U, Urra X, Planas AM. Neuroprotection in acute stroke: Targeting excitotoxicity, oxidative and nitrosative stress, and inflammation. *Lancet Neurol* 2016;**15**:869–81.
44. Xiong XY, Liu L, Yang QW. Functions and mechanisms of microglia/macrophages in neuroinflammation and neurogenesis after stroke. *Prog Neurobiol* 2016;**142**:23–44.
45. Liberale L, Gaul DS, Akhmedov A, Bonetti NR, Nageswaran V, Costantino S, et al. Endothelial SIRT6 blunts stroke size and neurological deficit by preserving blood–brain barrier integrity: A translational study. *Eur Heart J* 2020;**41**:1575–87.
46. Shao J, Yang X, Liu T, Zhang T, Xie QR, Xia W. Autophagy induction by SIRT6 is involved in oxidative stress-induced neuronal damage. *Protein Cell* 2016;**7**:281–90.
47. Stonesifer C, Corey S, Ghanekar S, Diamandis Z, Acosta SA, Borlongan CV. Stem cell therapy for abrogating stroke-induced neuroinflammation and relevant secondary cell death mechanisms. *Prog Neurobiol* 2017;**158**:94–131.
48. Jiang H, Khan S, Wang Y, Charron G, He B, Sebastian C, et al. SIRT6 regulates TNF- α secretion through hydrolysis of long-chain fatty acyl lysine. *Nature* 2013;**496**:110–3.
49. Yang F, Zhou L, Wang D, Wang Z, Huang QY. Minocycline ameliorates hypoxia-induced blood–brain barrier damage by inhibition of HIF-1 α through SIRT-3/PHD-2 degradation pathway. *Neuroscience* 2015;**304**:250–9.
50. Liu J, Zhang Z, Li X, Chen J, Wang G, Tian Z, et al. Forkhead box C1 promotes colorectal cancer metastasis through transactivating ITGA7 and FGFR4 expression. *Oncogene* 2018;**37**:5477–91.
51. French CR, Seshadri S, Destefano AL, Forname M, Arnold CR, Gage PJ, et al. Mutation of FOXC1 and PITX2 induces cerebral small-vessel disease. *J Clin Invest* 2014;**124**:4877–81.
52. Fatima A, Wang Y, Uchida Y, Norden P, Liu T, Culver A, et al. Foxc1 and Foxc2 deletion causes abnormal lymphangiogenesis and correlates with ERK hyperactivation. *J Clin Invest* 2016;**126**:2437–51.
53. Li D, Hu J, Wang T, Zhang X, Liu L, Wang H, et al. Silymarin attenuates cigarette smoke extract-induced inflammation via simultaneous inhibition of autophagy and ERK/p38 MAPK pathway in human bronchial epithelial cells. *Sci Rep* 2016;**6**:37751.
54. Xia S, Qu J, Jia H, He W, Li J, Zhao L, et al. Overexpression of Forkhead box C1 attenuates oxidative stress, inflammation and apoptosis in chronic obstructive pulmonary disease. *Life Sci* 2019;**216**:75–84.
55. Filippakopoulos P, Knapp S. Targeting bromodomains: Epigenetic readers of lysine acetylation. *Nat Rev Drug Discov* 2014;**13**:337–56.
56. Narita T, Weinert BT, Choudhary C. Functions and mechanisms of non-histone protein acetylation. *Nat Rev Mol Cell Biol* 2019;**20**:156–74.
57. Shen Y, Wei W, Zhou DX. Histone acetylation enzymes coordinate metabolism and gene expression. *Trends Plant Sci* 2015;**20**:614–21.
58. Jones BA, Varambally S, Arend RC. Histone methyltransferase EZH2: A therapeutic target for ovarian cancer. *Mol Canc Therapeut* 2018;**17**:591–602.
59. Singh PK. Histone methyl transferases: A class of epigenetic opportunities to counter uncontrolled cell proliferation. *Eur J Med Chem* 2019;**166**:351–68.
60. Crea F, Fornaro L, Bocci G, Sun L, Farrar WL, Falcone A, et al. EZH2 inhibition: Targeting the crossroad of tumor invasion and angiogenesis. *Canc Metastasis Rev* 2012;**31**:753–61.
61. Brand M, Nakka K, Zhu J, Dilworth FJ. Polycomb/trithorax antagonism: Cellular memory in stem cell fate and function. *Cell Stem Cell* 2019;**24**:518–33.
62. Yang J, Tian B, Brasier AR. Targeting chromatin remodeling in inflammation and fibrosis. *Adv Protein Chem Struct Biol* 2017;**107**:1–36.
63. Penas C, Navarro X. Epigenetic modifications associated to neuroinflammation and neuropathic pain after neural trauma. *Front Cell Neurosci* 2018;**12**:158.
64. Kaluski S, Portillo M, Besnard A, Stein D, Einav M, Zhong L, et al. Neuroprotective functions for the histone deacetylase SIRT6. *Cell Rep* 2017;**18**:3052–62.